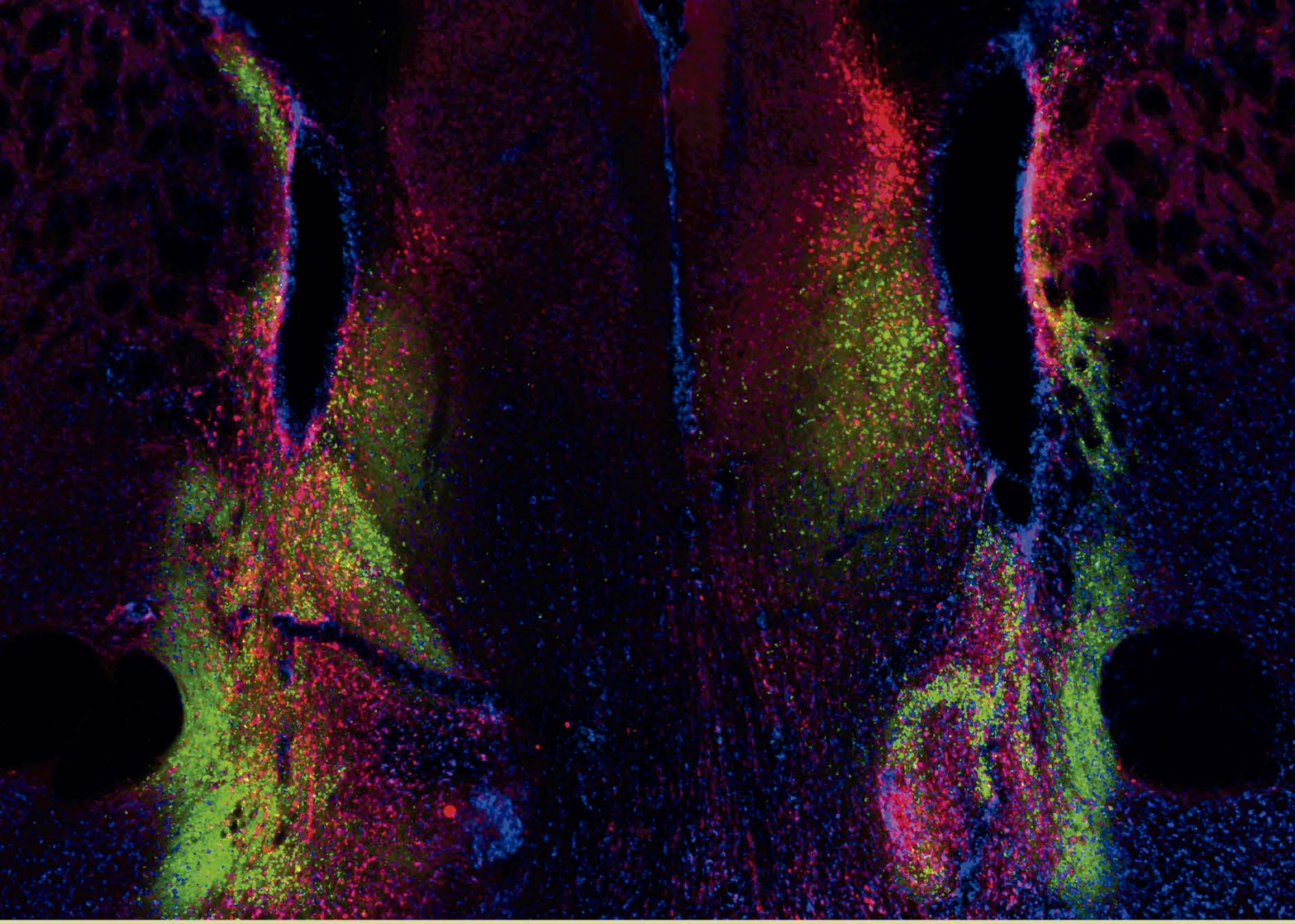

Tiago João dos Santos Reis

The role of cortico-striatal circuits in social hierarchies

Dissertação de mestrado em Biologia Celular e Molecular com especialização em Neurobiologia

Setembro 2017

· U C ·

Universidade de Coimbra

The role of cortico-striatal projections in social hierarchies

O papel das projeções cortico-estriatais em hierarquias sociais

Dissertação de mestrado em Biologia Celular e Molecular com especialização em Neurobiologia, orientada por João Peça e Ana Luísa Carvalho e apresentada ao Departamento de Ciências da Vida da Universidade de Coimbra

Tiago João dos Santos Reis

Coimbra, 2017

This work was developed in the following institution:

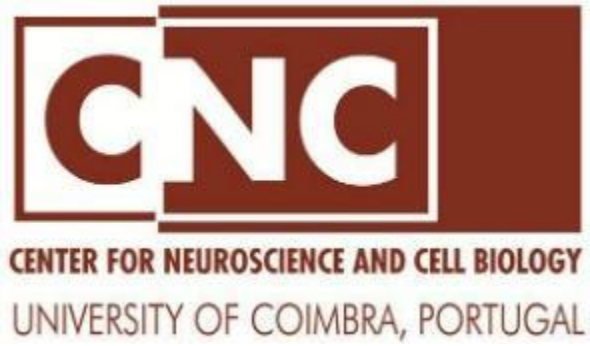

At the Neuronal Circuits and Behavior Group -
Center for Neuroscience and Cell Biology, University of Coimbra

This work was supported by the Portuguese Foundation for Science and Technology (FCT) and FEDER/COMPETE with FCT grants Pest-C/SAU/LA0001/2013-2014, BrainHealth 2020 (CENTRO-01-0145-FEDER-000008); work presented here was supported with grants award to João Peça from the FCT Investigator Program (IF/00812/2012), Marie Curie Actions (PCIG13-GA-2013-618525), Bial Foundation grant 266/16, the Brain & Behavior Research Foundation and FCT grant PTDC/NEU-SCC/3247/2014."

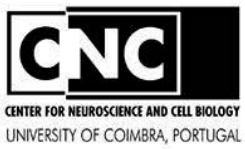

“In the midst of chaos, there is also opportunity”

— Sun Tzu, The Art of War

Agradecimentos

Em primeiro lugar, gostaria de agradecer ao Doutor João Peça por me ter aceite no seu laboratório e cedido a oportunidade de realizar um trabalho que me permitiu manipular técnicas avançadas, quase ao nível de "ficção cientifica". Para além disso agradeço lhe por todo o apoio e desafios colocados. Devido às minhas fracas projeções cerebrais entre regiões que coordenam planeamento de tempo, queria também especialmente agradecer pela completa prontidão que mostrou em corrigir-me a tese completamente em cima da hora e em época de férias.

Agradeço imenso à Lara que me impulsionou no inicio deste projeto e que sem ela não teria chegado onde cheguei.

A todos os membros do Neuronal Circuits and Behavior Group, Joana Guedes, Mohamed Edfawy, Mário Carvalho, Marcos Gomes, Catarina Seabra, Renato Sousa/João Calmeiro (<3) e a Marta Pereira, por todas as discussões cientificas e não cientificas e por me ensinarem como é/como se deve estar num laboratório, um profundo obrigado!

Ao Burger King™, *if you ask us, (chomping nosies) it just tastes better (chomp!).* totally not an ad though

Aos meus colegas de casa; a "mansão dos firmes" é um estado de espirito e num apenas um local. São as memórias e os laços de amizade que aqui formamos que vão ficar para a vida. Espero, no entanto, que nunca mais tenha que partilhar algum tipo de habitação com vocês.

Quick shoutout à Marta Pereira por ter feito a paginação e a tabela de conteúdos desta tese. Sem ela, a tese iria ficar confusa quando a imprimisse e depois ia ser o cabo dos trabalhos para a orientar outra vez.

A todos os meus colegas e amigos de licenciatura e mestrado que passaram, estão a passar e passarão por este processo. Pelos estudos intensivos, festas e jantares, pelos gritos académicos. Por nos mantermos unidos e falarmos como um só. Por sermos os melhores a todos os níveis, um obrigado!

"Queria também agradecer a minha e única namorada, sem o apoio dela nada disto teria acontecido! Por todas conversas, risos e desabafos, vou te estar eternamente agradecido!" Isto era o que eu gostaria de escrever, mas ela é um ser humano horrível, o que te safa é que és super gira.

Finalmente, quero agradecer às pessoas mais importantes na minha vida, a minha família. Nada disto teria acontecido sem vocês, por várias razões. Primeiro, vocês geraram me biologicamente, so there´s that. Segundo, o meu percurso até agora não teria sido possível sem vocês porque não teria dinheiro para pagar propinas, rendas e esses afins. No refunds though. Terceiro, por todo o apoio que me deram; todas as vezes que diziam "não sei a quem sais assim" e "não sei onde falhei", bem como todos os "não o conheço, deve ser estrangeiro" cada vez que alguém perguntava quem eu era. Ahah, clássico pais. Por tudo isto, MUITO OBRIGADO!

Contents

Abbreviations

Cg1 - Anterior Cingulate

ChR2 – ChanelRhodopsin

dmPFC – dorso medial Prefrontal Cortex

DV – Dorso-Ventral

Ephys – Electrophysiology

fMRI – functional magnetic resonance imaging

IL – Infralimbic

IT – Intratelencephalic

LFP – Local Field Potential

MEA – Multi Electrode Array

ML – medio-lateral

mPFC – medial Prefrontal Cortex

NAcc – Nucleus Accumbens Core

PET - Positron emission tomography

Prl – PreLimbic

PT - pyramidal tract

RC – Rostro-caudal

Abstract

In nature, animals in a group will engage in competition for dominance, leading to the formation of a hierarchy. A social hierarchy allows some individuals (of higher rank) to gain priority in accessing food, mate selection and resting places, reducing both the number and intensity of conflicts. Recent neuroimaging studies have begun to elucidate the neurobiological underpinnings of social hierarchy formation, by identifying and characterizing key brain regions involved in behavior repertoire. Furthermore, cortical projections between the mPFC (medial PFC) and Nucleus Accumbens (NAc) have been widely described to guide mice behaviour during non-social and, more recently, during social contexts. However, little is known about their role in social dominance behaviour.

In the course of this work, we found evidence that suggest that these two regions may encode winning information in the tube test setting. Furthermore, we were able to disrupt an already established social hierarchy by optogenetically activating corticostriatal projections, making the subordinate become dominant. Furthermore, we also found evidence that suggest that this change in rank can induce a "winner effect" in the stimulated mouse, winning trials even when not stimulated. However, this change was not long lasting, with the stimulated mouse returning to its initial rank after only a few days. Taken all into account, we provide further insight into the role of these projections and their involvement in social dominance behaviour.

Keywords: social hierarchy, medial prefrontal cortex (mPFC), nucleus accumbens (NAc), corticostriatal projections, optogenetics, In Vivo Electrophysiology

Resumo

Na natureza, animais que vivem em grupo envolvem-se em competições por dominância, levando à formação de uma hierarquia. Esta hierarquia social permite que alguns indivíduos (de maior estatuto) ganhem prioridade de acesso a alimentos, seleção de parceiros e lugares de repouso, levando a uma redução tanto no número como na intensidade de conflitos. Estudos neurológicos recentes, usando técnicas de imagiologia, começaram a elucidar os fundamentos neuronais da formação da hierarquia social, identificando e caracterizando as principais regiões cerebrais envolvidas neste tipo de comportamento. Além disso, as projeções corticais entre o mPFC (PFC medial) e o Nucleus Accumbens (NAc) foram amplamente descritas por orientar murganhos durante comportamento não social e, mais recentemente, durante contextos sociais. No entanto, pouco se sabe sobre o seu papel no comportamento de domínio social.

No decorrer desta tese, encontramos evidências que sugerem que estas duas regiões podem codificar o conceito de vitória durante o teste de dominância. Além disso, conseguimos perturbar uma hierarquia social já estabelecida ativando optogeneticamente estas projeções corticostriatais, fazendo com que o subordinado se tornasse dominante. Além disso, também encontramos evidências que sugerem que esta mudança de classificação pode induzir um "efeito vencedor" no murganho estimulado, levando à vitória de testes mesmo quando não estimulados. No entanto, esta mudança não foi duradoura, com o murganho estimulado regressando à sua classificação inicial após apenas alguns dias. Tendo em conta isto, nós aprofundamos o nosso conhecimento sobre o papel destas projeções e seu envolvimento no comportamento de dominância social.

Palavras-chave: Hierarquia social, córtex pré-frontal medial (mPFC), nucleus accumbens (NAc), projeções corticostriatais, optogenética, eletrofisiologia in vivo

Chapter I | Introduction

Social Hierarchy

In nature, most animals form social groups which lead to pairwise engagements and competition at the individual level [1]. While these challenges are performed to gain preferential access to limited resources [2,3] and mating opportunities [4], constant fighting is expensive in terms of time and energy [5]. As such, perpetual fighting for resources is not a viable option. To overcome this, a dominance hierarchies have emerged in nature as a structure between members of the same group to determine which individuals get priority of access, while also leading to a reduction in aggression and overall increase in group fitness [1,5].

In vertebrates, social stratification was first observed by Thorleif Schjelderup-Ebbe in 1921. Ebbe noticed that within a group of domestic fowls, some individuals (dominants) had priority in accessing food, resting places and selecting sexual partners. This stratification of access was named, by him a "Pecking Order" since fowls achieved dominance by pecking other fowls with their beaks [6]. Since then, it is now widely accepted that the dominance hierarchy and social stratification is a universal phenomenon among social animals, ranging from insects and fish, to rodents and primates [7].

Several factors, both intrinsic and extrinsic, may play a role in determining the outcome of these dominance competitions. *Intrinsic* characteristics may range from size, where bigger individuals usually have advantage during aggressive-submissive encounters; age, where in most primate societies older primates occupy top ranks; kinship, where the descendants of high-rank mothers (primates) often belong to the same rank as their mothers, with the possibility of moving upwards if they are males; gender, where males are usually more dominant than females, with exception for just a few species (e.g. hyenas); to personality, where timidity is associated with subordination [7]. *Extrinsic* factors are mostly serendipitous. For instance, facing a fatigued higher-ranked opponent in a critical dominant-subordinate encounter may lead to the victory of the otherwise subordinate. Additionally, the history of previous engagements may also be considered an extrinsic factor. Together, this suggests that social hierarchy formation follows a nonlinear path as it results from a combination of both individuals' intrinsic factors and non-deterministic conditions [7].

Once dominance-submission relations are settled, social ranks tend to remain unchanged for relatively long periods of time [1], but may be revisited each time a dominant animal is challenged by a lower rank individual. However, dominant members of the group do not benefit exclusively from perks and subordinate from drawbacks. While being the dominant party has advantages in higher reproductive success [8–10] and first access to food resources [2,3], there are several downsides. The most

common being higher metabolic rates and higher propensity for injury, as seen in pied flycatchers [11]. This can be due to the energetic costs of defending territory, mates, and other resources. Consequently, the individuals who spend more time in these activities, are prone to lose body mass over long periods of dominance [11,12] possibly leading to a decreased physical condition and eventual loss of ranking in the hierarchy [11].

Regarding subordinates, the same line of thinking may be applied. Although they may suffer from reduced access to nutrition [13,14] and decreased reproductive success [12,15], ultimately leading to a decreased fitness [16], there are a number of benefits to being subordinate. Knowledge of the pecking order [5] can be beneficial in agonistic conflicts where rank may predict the outcome of a fight where less injury will occur if subordinate individuals avoid fighting with higher-ranking individuals who would win a large percentage of the time.

Since dominance hierarchies are mainly established and maintained through physical strength and aggression [6,16], analyzing the levels of stress hormones present in dominant and subordinate animals has been thoroughly studied. In fact, in several species, it is the subordinate individuals who are more likely to suffer from higher levels of stress[17]. However, Sapolsky et al (2005) suggested that the correlation between these factors actually depends on the stability of the hierarchy and on specific societal characteristics, with high rank individuals experiencing the most stress in some particular scenarios and with subordinates being the most affected in others, as seen in **Table 1.**[16]

Table 1 – Effect of societal characteristics on stress incidence along ranking; * rank-related tendency; Adapted from Robert M. Sapolsky [16]

Societal characteristic	Individuals experiencing the most stress
Dominance style and means of maintaining despotic dominance	
Despotic hierarchy maintained through frequent physical reassertion of dominance	High-ranking
Despotic hierarchy maintained through intimidation	Low-ranking
Egalitarian hierarchy	*
Style of breeding system	
Cooperative	High-ranking
Competitive	*
Stability of ranks	
Unstable	High-ranking
Highly stable	Low-ranking
Availability of coping outlets for subordinates	
High availability	*
Low availability	Low-ranking
Ease with which subordinates avoid dominant individuals	
Easy avoidance	*
Difficult avoidance	Low-ranking
Availability of alternative strategies to overt competition	
Present	*
Lacking	Low-ranking
Personality	
Dominants perceive neutral interactions as challenging; subordinates take advantage of coping strategies	High-ranking
Dominants are adept at exerting social control and highly affiliative; subordinates are poor at exploiting opportunities for coping and support	Low-ranking

Study of Social Hierarchy in the Laboratory

Mice display highly adaptive social behaviour [18], best observed in the wild when there is adaptation to population density [19]. This social plasticity can also be observed in the laboratory setting since mice in captivity develop a strict social hierarchy due to the restraints of the home-cage. The stability of the hierarchy can decrease with an increased number of mice per cage [20] or when new objects are introduced, likely due to the objects being interpreted as a novel resource in need to be defended [21].

However, most studies of this social behaviour in the laboratory have been limited to brief dyadic interactions occurring in a context separate from the home-cage environment [22,23]. One of those dyadic interactions is the tube test, developed as a paradigm to score social dominance in rodents [24]. In the tube test, mice or rats are trained to walk through a narrow tube a nonviolent conflict situation is produced when two rodents are allowed to enter the tube from opposite ends and meet in the middle. Since mice resist backing out towards a place they cannot see, the animal that forces the opponent to retreat is scored as the more dominant of the pair [25] (**Figure 1).**

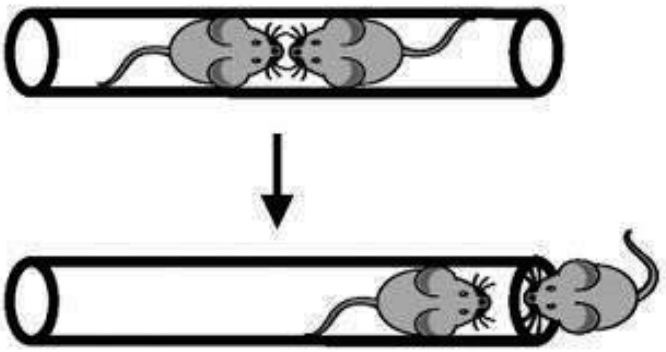

Figure 1 - Schematic of the tube test. Adapted from Fei Wang et al [25]

The observation that tube test winners are also dominant in other types of social behaviour, as seen in **Figure 2**, further supports the validity of the tube test as a measure of social dominance [25]. As such, applying a round-robin match arrangement, rank order can be determined for a large size of social group [25].

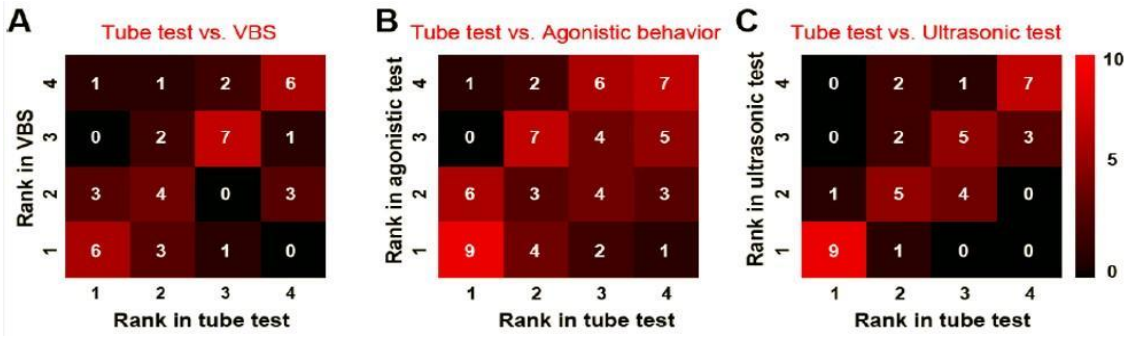

Figure 2 - Dominance in the tube test correlates with dominance in other Behavioral assays. Adapted from: Wang, F. *et al* [25]

However, new studies have suggested that these paired interactions alone cannot be account for the establishment of dominance hierarchies. The main argument in favor of this theory is that in nature, these interactions rarely occur in isolation [26,27]. Phenomena as the "audience effect" [27], the "observer effect" [28], and the "winner-loser effect" [29] can also intervene in the formation of these hierarchies in social groups.

Neuronal Circuits

Social hierarchy behaviour is dependent on a collection of cognitive traits that range from recognition of social status, learning of social norms, detection of violation of social norms, reading the intentions of others to monitoring reciprocal obligations [30]. As such, the neuronal circuits involved in the processing and control of behavioral responses during hierarchical clashes, is most likely complex.

Recently, Chiao et al (2010) and Zink et al (2008) performed a series of neuroimaging studies in humans, using functional magnetic resonance imaging (fMRI) (**Figure 3)**, where they were able to identify dissociable neural responses that respond to perceived social rank in an interactive, simulated social context [31,32]

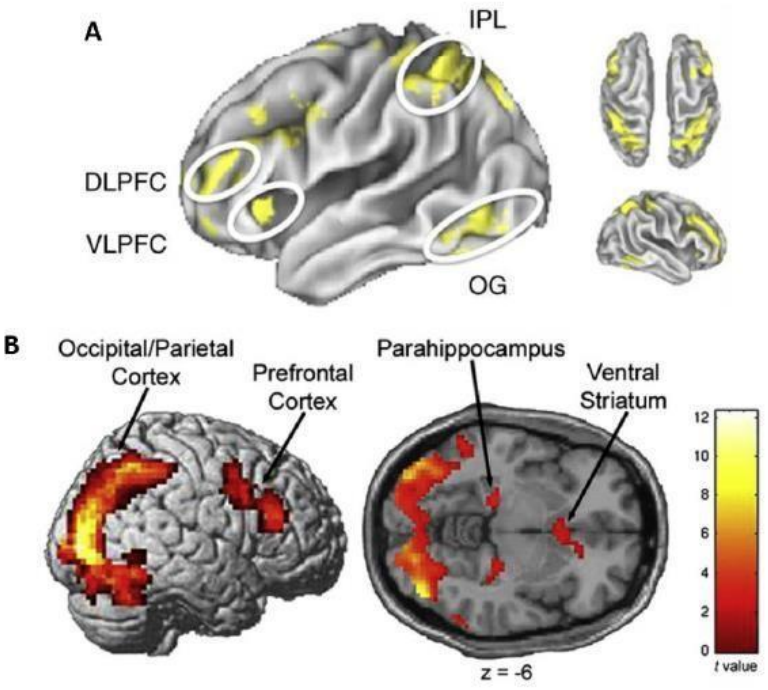

Figure 3 - (A and B) Brain areas significantly activated during social hierarchy perception **(A)** Adapted from Joan Y. Chiao [31] **(B))** Adapted from Caroline F. Zink et al [32]. Occipitotemporal gyrus = (OG), and inferior parietal lobe = (IPL), the dorsal and ventral lateral prefrontal cortices = (LPFC)

Furthermore, another recent study done in zebrafish by Chou et al (2016) showed that two subregions of the dorsal habenula antagonistically regulate the outcome of conflict and that such outcome reshapes the connectivity between them [33]. As this region is highly conserved across vertebrates, this data raises the interesting question if it is possible to manipulate neuronal circuits that govern innate social behaviors [34].

Taking all of this together, we are able to narrow down a few brain regions involved in the social behavior of hierarchy. Taking off from the findings from Chou et all, further research is required to determine if this type of connectivity between other brain regions plays any role in the observed social behavior and if specific Individual differences in how these brain regions are connected might promote an individual to seek a more or less dominant role in the hierarchy.

Medial Prefrontal Cortex

One of these brain regions of interest as seen by Chiao et al (2010) and Zink et al (2008) [31,32] is the prefrontal cortex (PFC), this regions is rich in excitatory pyramidal cells and has a small population of inhibitory GABAergic interneurons. It is thought that most information related to social hierarchies is processed in the PFC, the center for executive behavioral control [35]. In fact, human patients suffering from prefrontal cortex lesions demonstrated severely impaired social behavior, with reduced processing of social status information[36–38], loss of sensitivity to social cues and insensitivity to future consequences [39], despite having normal basic cognitive abilities [40]. The same can be observed in rodents, where lesions in the mesial prefrontal cortex, for example, lead to subordinate behaviour correlated with a low social rank[41], while lesions in the medial PFC (mPFC) lead to decreased interest, loss of social memory and a deficit in effort-based decision-making[42].

Moreover, the dorsal medial prefrontal cortex (dmPFC) is also shown to be involved in reasoning about other's mental states [43–45], accuracy during social cognition[46,47] and with the formation of impressions of people [48]. In addition, Wagner et al (2016), using fMRI showed that, when watching a movie, the human dmPFC is predominately activated when scenes involving social interactions between characters appear, in contrast with regions of the inferotemporal and parietal cortex that showed more activity to displays of faces and actions [49].

Furthermore, Zink et al (2008) have also demonstrated that, when in an unstable hierarchy setting, the medial PFC (mPFC) is activated [32], as seen in **Figure 4**.

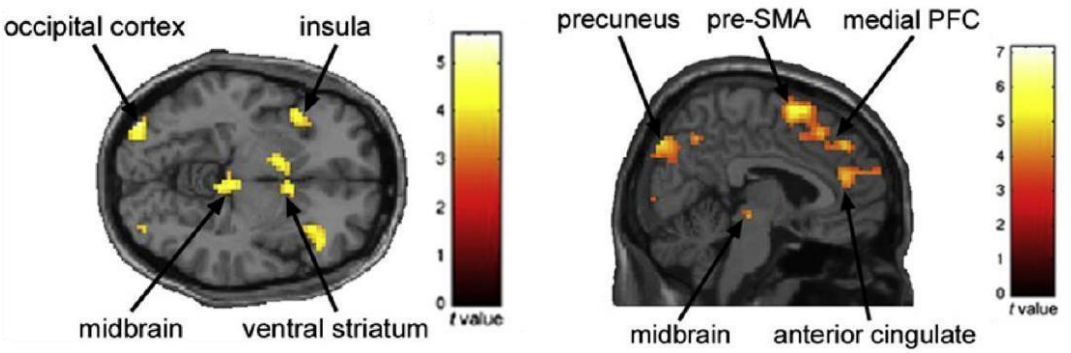

Figure 4 - Brain areas significantly activated in an unstable hierarchy setting. Adapted from Caroline F. Zink et al [32]

By representing an unstable hierarchy, this paradigm allowed participants upward and downward transitions across the hierarchy (positive and negative values respectively), mimicking what happens during hierarchy formation. This data further validates the PFC as a center responsible for determining a subject's relative social place in a hierarchy and as such, to be a key region involved in social hierarchy behavior.

On a more cellular level, Wang et al (2011), demonstrated that, by manipulating the mouse mPFC excitatory synapses, one could alter a previously established dominance rank, suggesting that social rank is plastic [25]. The same group, in a recent study using the tube test paradigm, found that a specific subset of dmPFC neurons fire when the animal is pushing the opponent and/or when he is resisting an opponent's push. Furthermore, they also demonstrated that optogenetic activation or inhibition of the dmPFC induced instant winning or losing, respectively[50]. Another study by Lee et al (2016), found that when approaching a stranger mouse in a modified version of the three-chamber test, a specific subset of mPFC neurons had a higher fire rate than normal[51]. Taken all of these results together, there is a clear body of evidence indicating that the mPFC plays a key role in social behavior.

One of these possible roles is that the mPFC may act as a mediator, planning actions based on available information and the internal state of the animal [52,53]. As such, the mPFC would receive inputs from other brain regions carrying information about the current situation, which would then compare it with previous similar encounters and, based on the learning outcome of those experiences, activate downstream regions for actions that were proven to be beneficial [54] **Figure 5.** As such, the mPFC may act as a central regulator, where the downstream brain regions are the effectors for social behaviour.

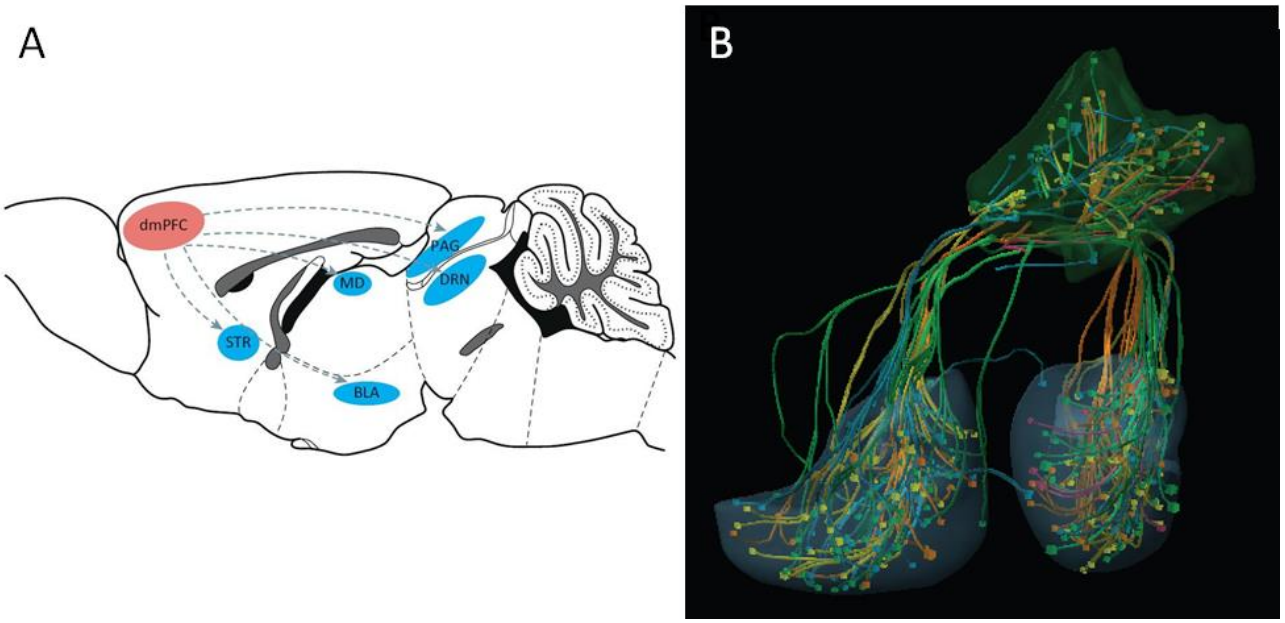

Figure 5 – (A) Potential neural pathways of social dominance downstream of the mPFC. Abbreviations: BLA, basolateral amygdala; dmPFC, dorsomedial prefrontal cortex; DRN, dorsal raphe nucleus; MD, mediodorsal nuclei of thalamus; PAG, periaqueductal grey; STR, striatum. Fei Wang et al [54] **(B)** Corticostriatal Projections designed in Allen Brain Explorer, kindly provided by Mário Carvalho.

Following this hypothesis, Felix-Ortiz et al (2015) found that optogenetic activation of Basolateral Amygdala inputs to the mPFC produced anxiogenic effects in the elevated-plus maze and open-field test, ultimately leading to a reduction of social interaction in the resident-intruder test. In contrast, inhibition produced anxiolytic effects, leading to a facilitation in social interaction. These results establish a relationship between the bidirectional modulation of anxiety and social behaviors [55] and further supporting the hypothesis that mPFC projections to downstream circuits play a key role in social behaviour.

Striatum

Another downstream brain region for mPFC efferentsis the striatum**,** which is known to code value, saliency, and reward-prediction-error signals [56–58]. The striatum is subdivided into ventral and dorsal striatum, with the ventral region being a limbic and associative related area and the dorsal region being a sensorimotor related area [59].

Zink et al (2008), using a reaction time task and fMRI, showed that the ventral striatum was significantly more active when viewing the face of a higher-ranked opponent in comparison with the face of a lower-ranked one, both when fighting a human or a computer player context. This specific

ventral striatum activity can be due to the assignment of a greater value to a higher-status player. Furthermore, they also showed that the striatum was most active when participants were told if they won or lost and when they defeated a superior human player, but not a computer one[32.] Taken together, these data further suggests that people are highly sensitive to rewards in competitive social situations [60,61] and that context-specific activity in the striatum can reflect motivational differences in different social scenarios[32].

Moreover, striatal activity may also be modulated by the subjects current emotional state and by what he/she stands to gain or lose [62–64]. Accordingly, Ly et al. (2011), using the MacArthur Scale of Subjective Social Status and fMRI, found that striatal activity was directly correlated with the social status of the test subject and the stimulus, where high-status individuals had a greater striatal response to high-status information and vice-versa [65], as seen in **Figure 6**.

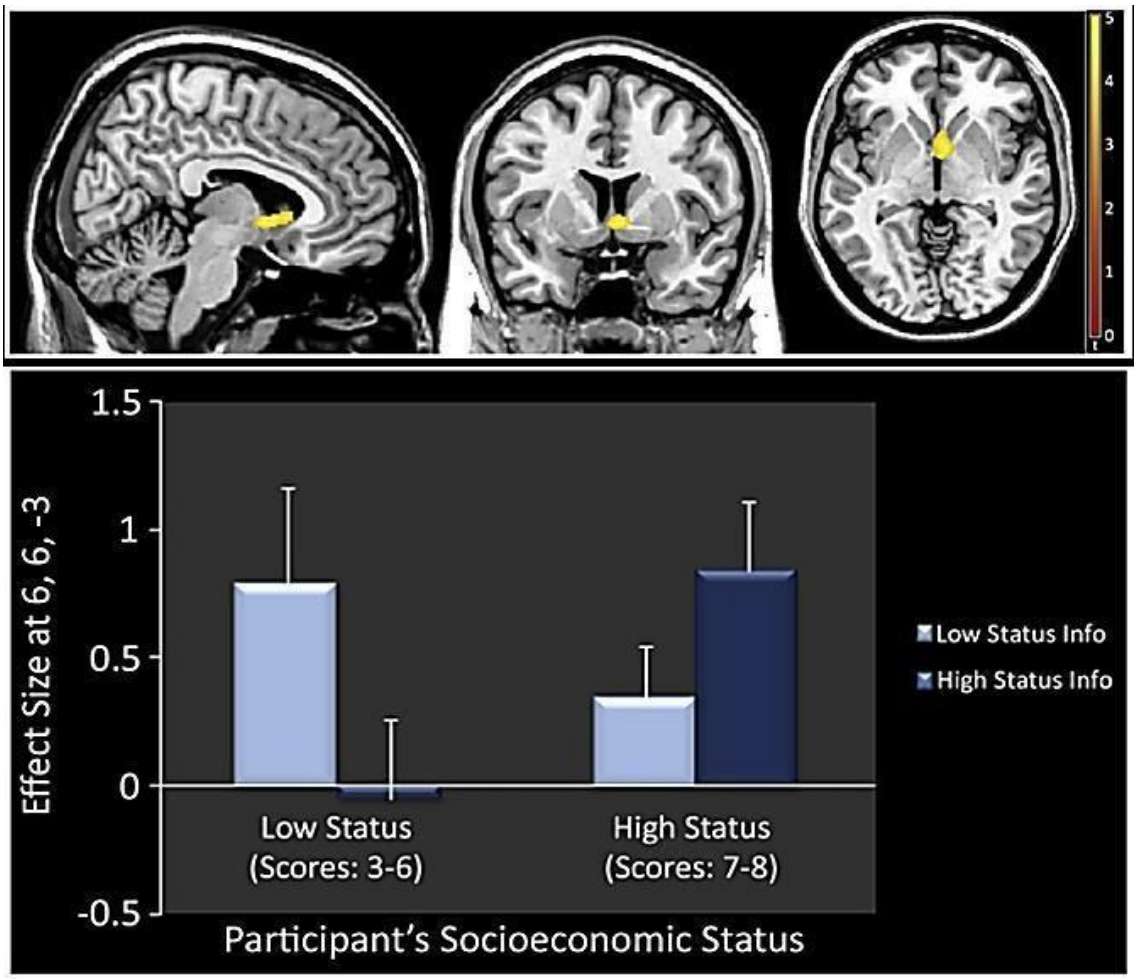

Figure 6 – Ventral striatal response to low and high rank information, accordingly to subject's social economic status; Adapted from Martina Ly et al [65]

Furthermore, Drake Morgan et al (2002), using Positron emission tomography (PET) in cynomolgus monkeys, showed that, after three months of social housing, animals that became dominant expressed significantly more D2/D3 receptors on the striatum in comparison with subordinates and than when individually housed. Moreover, no significant changes were seen in the expression of the same receptors in subordinates [66], as seen in **Figure 7.** Furthermore, another recent study performed in macaque monkeys by Báez-Mendoza and Schultz (2016) showed that striatal neurons signal performance errors [67]. This data further supports the involvement of the striatum in social hierarchy-related behavior.

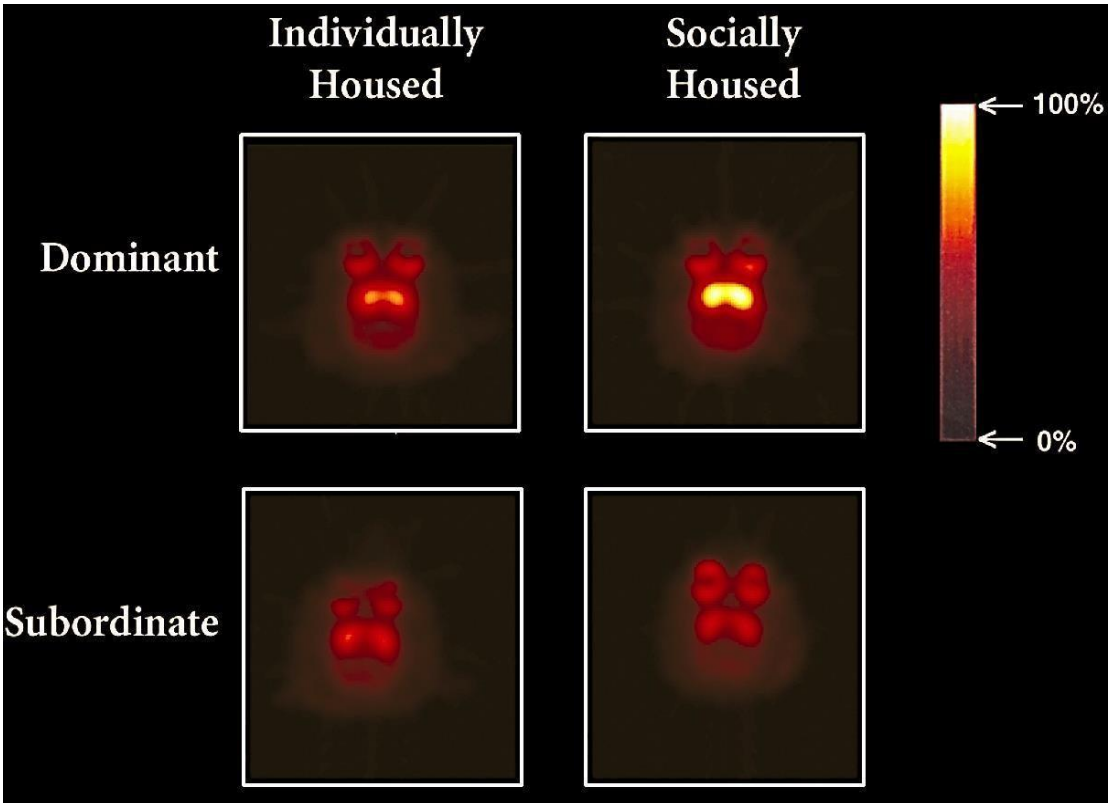

Figure 7 – [^{18}F] FCP dopamine D_2 receptor labelling in the basal ganglia of individually and socially housed dominant and subordinate cynomolgus monkeys; Adapted from Drake Morgan et al [66]

When taken all of these data together, and although the PET studies are not a direct indicative of striatal activity, it allows us to infer that the striatum plays a key role in social hierarchical behaviour and thus, it is an interesting target to study any possible cortico-striatal projections and their role in this behaviour.

Corticostriatal projections

Neural connectivity between the cortex and striatum regions is accomplished through the commonly designated corticostriatal projections, in a well-defined directionally arranged wiring pattern: cortex communicates monosynaptically to striatum, whereas the striatum communicates only indirectly to cortex via polysynaptic complementary circuits [68–71]. This specific organization seems to be directly correlated to the corticostriatal system's roles in cognitive and motor functions.[59,68,72]

Regarding the spatial map of the corticostriatal connectivity (i.e. which brain regions project to where), a very distinct ventromedial-to-dorsolateral topography can be seen in mice **(Figure 8).** The Infralimbic (IL) and the ventral part of the Prelimbic regions project to the most ventromedial portion of the striatum, named nucleus accumbens (NAc) shell (AcbS). The remaining portions of the PL and the ACG project towards the core of the NAc (AcbC) and then extend to the dorsomedial caudate-putamen complex of the striatum. Lastly ACG and AGm project to the dorsocentral part of the caudate-putamen complex [59] .

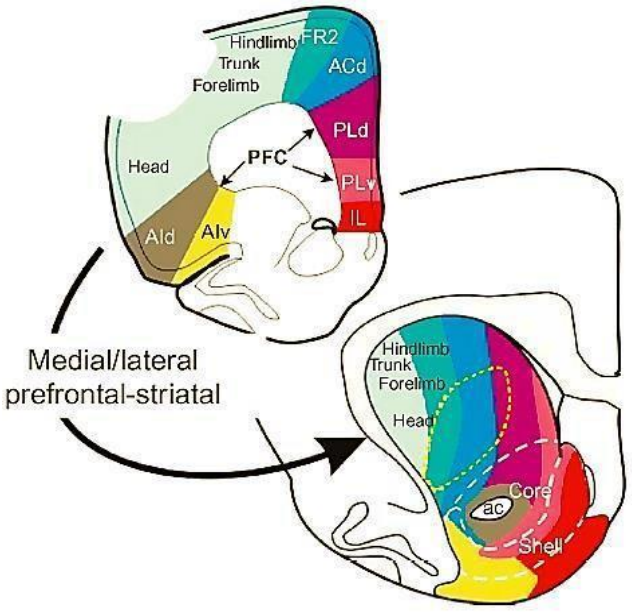

Figure 8 - Coticostriatal hodology topography; PFC, prefrontal cortex; AId, dorsal agranular insular cortex; AIv, ventral agranular insular cortex; FR2, frontal area 2 (also known as medial agranular → AGm); ACd, dorsal anterior cingulate; PLd, dorsal prelimbic cortex; PLv, ventral prelimbic cortex; IL, infralimbic cortex; ac, anterior commissure; Adapted from Henk J. Groenewegen and Harry B. M. Uylings [81]

At a more cellular level, the corticostriatal system is comprised by two different classes of cortical neurons, the Intratelencephalic (IT) and the pyramidal tract (PT) neurons, each one having its

own set of characteristics[73]. For instance, IT neurons are placed across several layers of the cerebral cortex, going from layer 2 up to layer 6, with only the neurons from layers 5A, 5B and 6 projecting bilaterally to the striatum only, never leaving these two regions. As such, they're called intratelecenphalic. PT neurons also innervate the striatum but, unlike the IT neurons, only project from one cortical layer 5B and cannot cross to the contralateral hemisphere, as such the striatum receives inputs from both types of neurons coming from layer 5B [68]. However, PT neurons also project to several regions outside the telencephalon, such as the thalamus, subthalamic nucleus, midbrain and others, ultimately reaching the brainstem and spinal cord regions[68,71,74]. Further studies have also revealed that IT and PT neurons cross-talk in the cortex, with information generally going in the IT → PT direction[75–77], which suggests that PT neurons locate downstream within the cortical circuit. It is otherwise proposed that corticostriatal projections obey this well-defined hierarchical transmission as a way of amplifying, integrating, distributing and storing information within subsets of neurons[78–80].

These two neuron types, however, differ in the information they convey to striatum, with IT-type neurons conveying sensory and motor planning information and PT-type neurons conveying motor commands. Furthermore, the IT-type neurons preferentially target the direct pathway while the PT-type neurons preferentially target the indirect pathway striatal neurons[81].

One interesting hypothesis arises from the fact that the PT neurons project to multiple regions. As such, these cells could be the ones responsible for controlling several different aspects of the dominance behaviour as they are able to target multiple regions simultaneously, meaning that their behavioural functions may derive from their combined output projections [68]. As such, this hypothesis can explain the altered social behavior seen by Wang et al (2011) by acting on just one region [25,50].

Furthermore, the fact that those researchers successfully manipulated a social hierarchy by modulating the excitatory output of the PL cortex [25,50], which principally innervates the core and shell of the Nacc, further supports the hypothesis that these ventromedial corticostriatal projections are involved in social hierarchy behavior.

Although these glutamatergic projections of the mPFC to the NAcc and shell have been well described and validated by optogenetic approaches [82,83], there is an interesting study done by Lee et al (2014) where they demonstrated the existence of long range GABAergic projections from the mPFC to the NAcc, indicating that not all GABAergic neurons residing in the mPFC are local

interneurons. Furthermore, they also demonstrated these neurons are capable of eliciting acute avoidance behaviour in a Real-time place preference test [84]. However, this data is only supported by a single study and as such, further work is required to completely characterize these projections.

Corticostriatal projections are already well described in the literature to be involved in guiding behaviour through different non-social prepositions, more specifically when linking behaviours across contexts is required[85] or to weight the costs and benefits of certain actions[86], including assessment of action consequence and potential rewards[87,88].

Furthermore, a recent study, done by Amadei et al (2017), showed that a rhythmic activation of this circuit within a social context can induce and accelerate a preference towards a partner, without the need for mating rituals. Importantly, this study successfully shows the recruitment of the brain's reward systems during social interactions, via the corticostriatal system, and, more importantly, implicate these projections during mice behaviour in social prepositions[89].

To sum, although a body of evidence is provided showing that the mPFC and the striatum are involved in social hierarchy behaviours and are anatomically and functionally connected, further studies are still needed to determine if these corticostriatal projections are specifically involved in this type of behaviour and if so, what role do they play in determining the social rank of the individual.

Specific objectives:

With this project, we intended to explore the circuits involved in social hierarchy by answering two main questions:

I. Are there any specific connections between the mPFC and the Striatum that are differentially active during social interactions?
II. If so, is it possible to manipulate these hierarchies by interfering with cortico-striatal projections?

Chapter II | Materials and Methods

Animals

Male C57/BL6 mice, 2-5 months old (Charles River) were used for all behavioral experiments. Animals were housed at the vivarium of the Faculty of Medicine at the University of Coimbra, in groups of 4 per cage with food and water provided *ad libitum,* and maintained in a 12 hours light/dark cycle in temperature- and humidity-controlled rooms. When arriving, animals acclimatize to the vivarium and daily routines for at least one week after which they were handled twice a week. Animal identification was performed by subcutaneous injection of green and/or black dyes in the paws. All experiments were carried with the approval of the animal ethics committee of the Center for Neuroscience and Cell Biology, University of Coimbra (ORBEA), the approval of the Portuguese DGAV and in accordance with EU directives regarding animal use in research.

Implantable Optical Ferrules

Custom-made implantable optical ferrules were constructed from 2.5 mm long 270 µm inner diameter ceramic stick ferrules (Thorlabs) based on a previously described design[90]. Briefly, a 200 µm diameter 0.39 numerical aperture optical fiber (Thorlabs) was stripped of its protective coating and cleaved, next, cyanoacrylate adhesive (Loctite) was applied to the concave end of the ferrule through which the cleaved fiber segment was threaded. After wiping off the excess glue, the ferrules were allowed to cure for 30 minutes at room temperature. The ferrule connector was polished using a polishing disk and increasingly fine grades of polishing paper (Thorlabs), with frequent inspection to ensure transmission quality. Once polished, the free end of the fiber was scored and cleaved to 2 mm in length. **See Supplementary Figure 1**

Multi Electrode Array (MEA)

A 12-channel MEA was designed by our lab and constructed by Microprobes for Life Science (USA). **See Supplementary Figure 2** The MEA consisted of two sets of electrodes, each containing 6 electrodes made from tungsten. The first set of electrodes was designed to reach the mPFC of the mouse, with the electrodes length ranging from 2,45 to 2,70 mm. The second set was designed to reach the NAcc, with the electrodes length ranging from 5 to 5,25 mm. The final impedance of the electrodes was between 500-1000 kΩ. A reference electrode was also present, outside of the two sets, with a length of 5,25 mm. Each electrode was separated from neighbouring electrodes by 0,25 mm.

Surgical procedures

For this thesis work, two different approaches were used for the bilateral delivery of an Adeno-associated viral construct coding for Channelrhodopsin (AAV-hSyn-hChR2(H134R)-EYFP) to the NAcc

and for the Optical Fiber implantation to the mPFC. The differences between Approach #1 and Approach #2 relied on the angle of insertion of both the glass micropipette carrying the AAV or the Optical Fiber stub, both of which will be further detailed below. Another set of surgeries were also performed with Evans Blue injection instead of the AAV for visual confirmation of the coordinates and technique used. The core of our procedure was largely based as described by Cetin et al (2016)[91], with some critical changes in order to accommodate to our specific requirements.

Preparation of surgical area and tools

Before starting the surgery, the surgical area was disinfected by wiping with 95% ethanol and the tools were sterilized by autoclaving or by immersion in disinfectant. Aseptic conditions were maintained to prevent infection.

Anesthesia and fixation of animal in stereotaxic apparatus

Animals were weighed and placed in a sealed chamber with a 5% isoflurane/0_2 mixture until they fully anesthetized. The animals were then transferred to a breather/nozzle with 2% isoflurane/0_2 mixture to maintain anesthesia. Next the fur on the animal head was shaved from between the eyes to behind the ears. The animals were transferred to the stereotaxic apparatus and their mouths carefully placed onto the incisor bar. To fix the animals in the apparatus, one ear bar was gently placed slightly above the animal's the ear canal and a second ear bar was slowly positioned to complete the fixation. Because this procedure involves recovery from surgery, only non-rupture ear bars with a wide angle tip were used to avoid injuring the tympanic membrane. After successful fixation, Meloxicam was administered Intraperitoneally (IP) (1 mg/kg), followed by 0.3 ml of 0.9% (wt/vol) NaCl IP. Ophthalmic ointment to eyes was maintained throughout the surgery to prevent drying.

Surgery (preparation of craniotomy)

To minimize the risk of infection, the animals skin was wiped with Betadine and alcohol. Using a scalpel, and with the assistance of a dissecting microscope at a low magnification (×10 to ×20) to visualize the top of the animal skull, a 1–1.5-cm incision was made through the midline of the scalp. Using surgical scissors or forceps, the subcutaneous and muscle tissue were separated to create a window wide enough that both the Bregma and the Lambda were seen clearly. A cotton swab was inserted into a 30% hydrogen peroxide solution and used to swab the skull to further expose cranial cranial sutures and aid in the identification of the bregma and lambda locations. The head of the animal was then levelled by measuring z coordinates of bregma and lambda and adjusting the head position so that both coordinates become plane. Furthermore, we also confirmed the head was level on the medio-lateral axis.

Craniotomy

Using the stereotaxic atlas (Paxinos, 1997), the brain region of interest and its coordinates were determined. Using a glass micropipette with the tip filled with gentian violet, these coordinates were marked onto the animal's skull for better visual guidance to the craniotomy procedure. To further increase the bond strength between the skull and the dental cement used for fixation of the Optical Fibers or the MEA, the skull was scored over the target area using a hand-held drill in horizontal movement and slight downward pressure. Afterward, the skull was drilled on the marked coordinates and using a small needle (26 G) the dura matter was removed. OctoColagen (Laboratorios Clarben SA) and small drops of Epinephrine (3M) were used to stop bleeding.

Injection of virus or Evans Blue

The injection micropipette was placed into the Nanoliter Injector (World Precision Instruments) and filled with 2 µl of the ChR2-coding AAV or Evans Blue (1%). The tip of the micropipette was brought to Bregma to re-calculate "Zero". The coordinates used for this procedure were RC: + 1.5 mm; ML: ± 0.8mm, while injecting at 3 different dorso-ventral coordinates, as follows: DV: - 4.3/- 4.0/- 3.7 mm. At this point, one of the two approaches described below was used for the placement of the glass micropipette. The rest of the procedure was similar, independently of the approach used.

"0 degrees angle" Approach

The micropipette was brought to the appropriate coordinates and lowered until it touched the brain surface. **See Supplementary Figure 3(B)**

"10 degrees angle RC" Approach

The micropipette was placed with an 10° angle and then brought to the appropriate coordinates and lowered until it touched the brain surface. **See Supplementary Figure 3(C)**

The cut tip of the micropipette has a sharp edge, to allow easy penetration of the brain. The craniotomy window was kept well hydrated with Saline throughout the all viral injection procedure. The micropipette was then lowered at a rate of ~1mm/min until it reached the first DV coordinate of - 4.3mm. After this coordinate was reached, we waited 5 minutes prior to injection. Afterwards, 2 injections, separated by 15 seconds, were performed delivering 69 nl of virus (3.38×10^{13} GC/mL titer) or Evans Blue solution. Afterwards, we waited 5 minutes before pulling the micropipette up at a rate of ~1 mm/min, until it reached the second DV coordinate of -4.0mm. The same procedure was applied

for this coordinate and for DV coordinate of - 3.7mm. After the last injection, we waited an additional 10 minutes before pulling the micropipette up, in order to prevent any possible leakage of virus to unwanted regions. After the micropipette was completely out, we proceeded to optical fibers implantation, where we used one of the two approaches described below for the placement of the Optical Fibers. The rest of the procedure was similar, regardless of the approach used (see below).

Optical fibers Implantation

"0 degrees angle" Approach

For the optical fiber implantation, the stereotaxic adapter for implantable optical fibers was attached to the stereotaxic arm and the optical fiber was aligned such that it is perpendicular to the skull. The coordinates used for insertion were RC: +1.8; ML: +0.5; DV: -1.6. **See Supplementary Figure 4(A)**

"10 degrees angle ML" Approach

For the optical fiber implantation, the stereotaxic adapter for implantable optical fibers was attached to the stereotaxic arm and the optical fiber was tilted to 10º outwards in the medio-lateral axis. The coordinates used for insertion were RC: +1.8; ML: +0.6; DV: -1.3. **See Supplementary Figure 4(B)**

The stereotaxic arm with the implantable optical fiber was then lowered into the brain region of interest at a rate of ~1.5 mm/min. The craniotomy window was kept well hydrated with saline throughout the all implant procedure.

Multi Electrode Array Implantation

Implantation of the MEA involved a slightly larger craniotomy and the drilling of four screw holes in the region between lambda and bregma, two in each hemisphere. For these surgeries, a 1.5 x 1.5 mm craniotomy was performed. After, the dura was completely removed with a small needle (26 G). OctaColagen (Laboratorios Clarben SA) and small drops of Epinephrine (3M) were used to stop any bleeding. With a glass micropipette filled with gentian violet, small points were marked in the brain surface to help visual guidance for the MEA implant procedure. Next, 4 stainless steel, sterile screws (M1.2) were implanted until contact with the dura and further fixated with VersaGlue PX-40 (Harvest Dental). The stereotaxic adapter for the MEA was then attached to the stereotaxic arm and the MEA aligned perpendicular to the skull. The stereotaxic arm with the MEA was then lowered into the brain region of interest at a rate of ~1 mm/min. The craniotomy window was kept well hydrated with saline throughout the all implant procedure. After reaching the final Z coordinate, a small drop of VersaGlue PX-40 (Harvest Dental) was placed at the top of the MEA for further fixation and left to dry for 10

minutes. Meanwhile, the Ground Wire was connected to the ground screw by wrapping it at least three times over and under itself.

Cement Application

Dental cement (Ketac Cem, 3M) was used to secure the Optical fibers or the MEA in place. Using a small brush or a toothpick, the dental cement mixture was applied throughout all the exposed skull and the implant. After verification that the implant is completely secured, a dental acrylic mixture was applied (Scheu Dental) to further secure the implant and to prevent possible damage done by the other mice in the cage environment.

Surgery Recovering

Mice were single housed for 1 day for recovery after surgery, before group housed again, with access to wet food and water mixed with minocycline (0.1mg/ml). Animals that were implanted with MEAs were given a single injection of Meloxican (1mg/kg) 18 hours after the surgery and Bupremorphine (0.1mg/kg) 24 hours after.

Behavioral tests

All experiments were performed in the light cycle (08h00 to 20h00) and animals were allowed to acclimatize to testing room environment for at least 1 hour prior to testing.

Tube test

Mice were housed in groups of 2 for at least 2 weeks before tube test. In two successive training days, each mouse was trained to go through a transparent plexiglass tube (33 cm in length, 3 cm in diameter) for 10 trials. For mice implanted with optic fibers and MEAs, a 12-mm slit was opened at the top of the tube. For the optogenetic manipulation experiments, each trial day consisted of 3 tube test trials except in trial days where photo stimulation was delivered, with these days ranging from 3 to 9 tube test trials. Acrylic ramps permitted the animals to easily access and retreat from the tube. Testing started by introducing two different subjects to the edges of the tube. Testing ended as soon as one of the subjects had all paws outside of the tube for at least 4 seconds. Introduction to the tube test entrance was randomized and balanced. Animals rested 24 - 48 hours between trials. Camera recordings were performed in side view and video-taping was scored offline using Cineplex Editor (Plexon). Dominance relationships were generated by determining the subject who leaves the tube as the subordinate in each particular dyad.

Tube test behavioral decoding

Videos of all the tube test trials were analyzed frame by frame using Cineplex Editor (Plexon). Observations begun at the time-frame immediately after tail-release of subjects and ended 4 seconds after an animal left the tube completely. Specific behaviors during the trial were categorized into pushing, stillness, resistance (both when pushing or being pushed) and retreating. Behavioral results were then aligned with electrophysiology data to acquire firing rates during various behavioral epochs. Mean firing rates of every neuron during each behavior epoch were then calculated and compared. All data regarding in vivo ephys was then analyzed using NeuroExplorer and Offline Sorter (Plexon).

Optogenetic manipulation of corticostriatal projections in the tube test

Photo stimulation was applied at least 4 weeks after viral injection and delivered by coupling an external optical fiber (200 µm in diameter, NA: 0.39) to the implanted optic fiber through a ceramic sleeve. LED-generated blue light pulses were delivered to the mPFC through the optical fiber implant, coupled to a 465-nm laser (PlexBright LED, Plexon). Stimulus parameters of the laser were controlled with a pulse generator (PlexBright LD-1, Plexon) connected to an Arduino board. On the photo stimulation days, tube test ranks were first measured without light, then with 465 nm blue light turned on right before mice entering the tube and kept on though the duration of the trial. 3 different protocols of photo stimulation were used during the duration of this thesis, each in their own set of animals. First, a bilateral, non-frequency modulated photo stimulation was delivered to the mPFC of the mice when both of the subjects were touching. Secondly, a bilateral, non-frequency modulated photo stimulation was delivered from the beginning to the end of the tube test trial. Lastly, a unilateral, non-frequency modulated photo stimulation was delivered from the beginning to the end of the tube test trial.

cFos Protocol and immunohistochemistry (IHC)

For c-fos induction, 1 min of photo stimulation (465 nm), followed by a 2 minutes wait, followed by another 1 min of photo stimulation, was delivered unilaterally to the dmPFC of mice injected with AAV-hSyn-hChR2(H134R)-EYFP virus. After 90 minutes, mice under isoflurane anesthesia were rapidly dissected to expose the heart. Next, 20 mL of ice-cold 1x phosphate-buffered saline (PBS) (10x PBS - 87,6 g of NaCl (Acros); 32,5 g of Na2HPO4.7H2O (Fisher); 4 g of KH2PO4 (Fisher) was perfused through the left ventricle. A cut in the atrium was done in order to allow the blood to exit circulation and eventually sacrifice the anesthetized animal by blood loss. Afterwards, 40 mL of fresh ice-cold 4% paraformaldehyde (PFA) (4% PFA - 4 g of PFA (Fisher); in 1x PBS) was perfused to fix the tissue. Dissection and removal of the brain was carried out and brain samples were then immersed in ice-cold 4 % PFA solution and left overnight at 4ºC. Samples were changed to a 4 % PFA solution

containing 30 % sucrose (30 g sucrose (Fisher); 100 mL of 4 % PFA) at 4 ºC, to further fix and preserve the tissue through an osmotic exchange. Brain samples were then sliced in the vibratome (Leica, Wetzlar, Germany) to generate 30 um thick slices. These were then repeatedly washed in 1 mL 1x PBS and incubated with blocking buffer (0,5 mL of 5 % goat serum (Thermo); 0,2 g of bovine serum albumin (BSA) (NZYTech); 20 uL of 0,2 % Triton-X 100 (Acros) at room temperature for 1 hour. Afterwards, slices were incubated with blocking buffer containing the primary antibody against cFos for 48 hours at 4 ºC. Additionally, after three wash steps, slices were incubated in blocking buffer with the secondary antibody overnight at 4 ºC and mounted with 4',6 -diamidino-2-phenylindole (Dapi) - containing mounting media (Mowiol 4-88, Sigma). Imaging was performed in the Axio Imager 2 microscope (Zeiss, Germany).

Electrophysiological Recordings

Mice housed in groups of 4 were implanted with the MEA as described above. After 1 day of isolated recovery, they were placed in group housing for 7 days. Mice were then trained daily in the home cage environment, isolated or in group housing, and in the tube test while being recorded with the MEA connected to the amplifier to get habituated with the recording procedure. The connecting wire was counterweighted to mitigate the effects of the apparatus on the animal's movement.

Data acquisition and analysis

Our in vivo ephys recording system was interfaced with behavioral tracking dat and neuronal data acquisition. A CinePlex V2 Digital Video Recording and Tracking System (Plexon Inc., Dallas, TX) coupled with an Imaging Source TM camera (640x480 resolution, 30 frames per sec) was used for tracking animals' location during behavioral performance. Neuronal activity recorded from the MEA was pre-amplified at the head stage level (HST/32V-G20-2LED32-channel VLSI headstage, 20x gain, 2 LED lights (red, blue, and green LEDs provided), Plexon, Inc., Dallas, TX). Single-unit activity was filtered between using a high-pass filter of 300 Hz and LFPs were filtered between 0.3–200 Hz. The signal was digitized at 40 kHz (Omniplex D system, Plexon).

Local Field Potential analysis

Spectrograms and Power Spectral Densities (PSD) were created using Neuroexplorer (Plexon). Spectrograms displayed frequencies from 0 to 100Hz, with 512 Frequency Values. Power was calculated as the Log of PSD (dB) and a Gaussian filter was applied to smooth the data. PSDs displayed frequencies from 0 to 100Hz, with 1024 Frequency Values. Power was calculated as the Raw PSD and a Gaussian filter was applied to smooth the data.

Chapter III | Results

Surgery Procedure Optimizations

To first assess if our set of brain coordinates and stereotaxic surgery procedure was correct, two sets of confirmation surgeries with Evans Blue injections were performed, as described in the Material and Methods section. The first set was performed using our "0 degrees" Approach, which is the traditional flat-skull technique (**Figure 9 and Figure 10)** and the second set was performed as described in "10 degrees" Approach (**Figure 11 and Figure 12).**

Regarding the "0 degrees" approach, although the target areas we were aiming for (mPFC and NAcc) were successfully reached, we could not observe a clear single straight trace of dye in any given slice observed. Instead, as observed in **Figure 9** in the black box**,** the glass micropipette tip started to appear from the top of the brain surface until it reached the brain region of interest, in an anterior-to-posterior manner, meaning that the descent was tilted in the rostro-caudal axis.

After searching the literature and with calculations based on our own data, we postulated the brain is slanted in relation to the skull at approximate 10-12º degrees. To corroborate our hypothesis, we performed a new set of surgeries but with a descent of 10° in the anterior-posterior axis, as described in **Supplementary Figure 3C**. As can be observed in **Figure 10A,** specifically in panels 2-4, and in in **Figure 10B**, specifically in panels 3-6, the "needle trace" was now clearly visible, indicating that our descent procedure was now perpendicular to the brains rostral-caudal axis. This updated angle of insertion consisted in the "10 degrees" Approach.

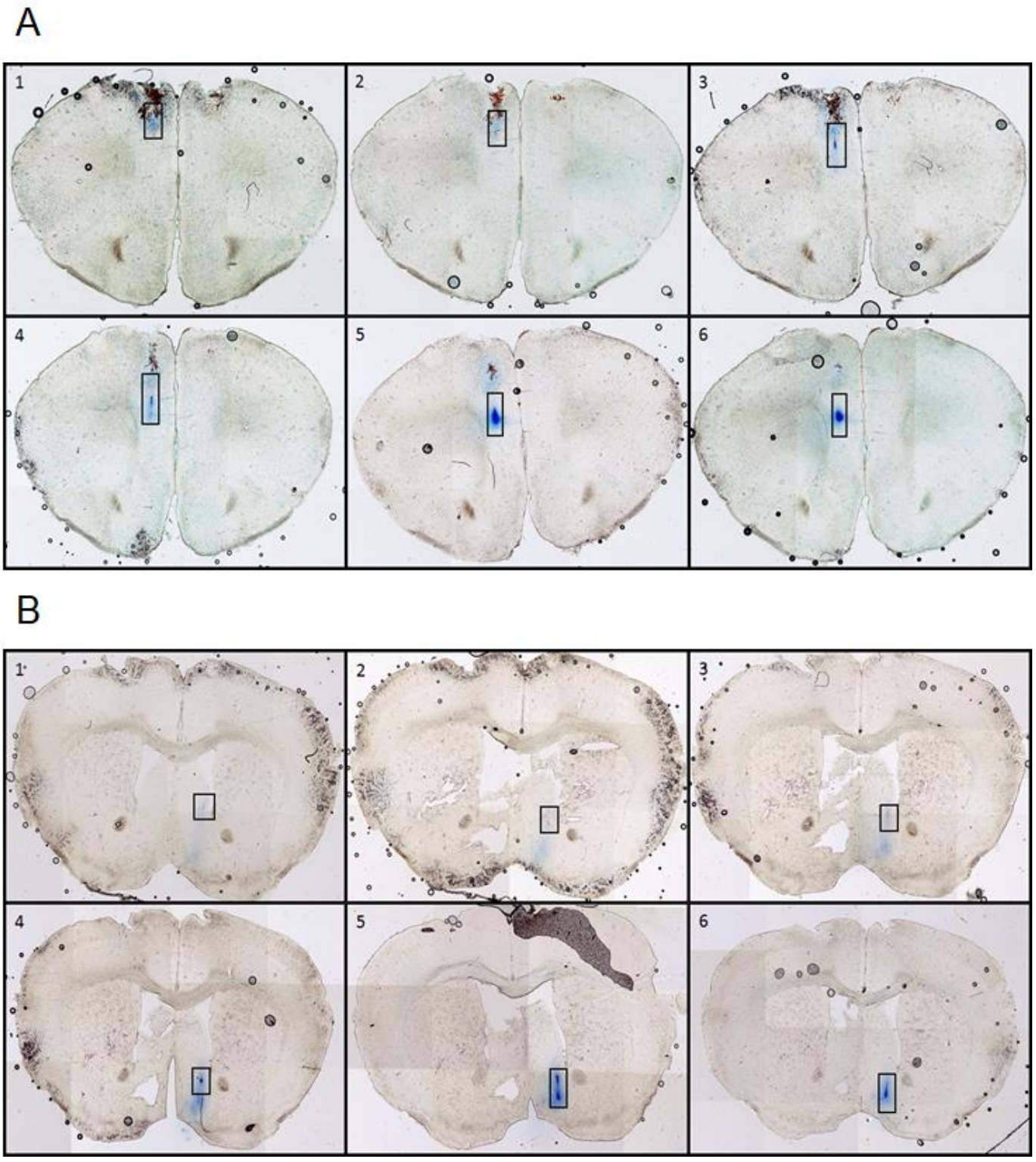

Figure 9 - Stereotaxic surgery with Evans Blue Injection 0º of inclination. (A) Anterior to posterior brain slices from a mouse injected with Evans Blue into the mPFC. **(B)** Anterior to posterior brain slices from a mouse injected with Evans Blue into the NAcc. The black box indicates the current position of the glass micropipette tip during its descent until reaching final DV coordinate. (n=3 animals)

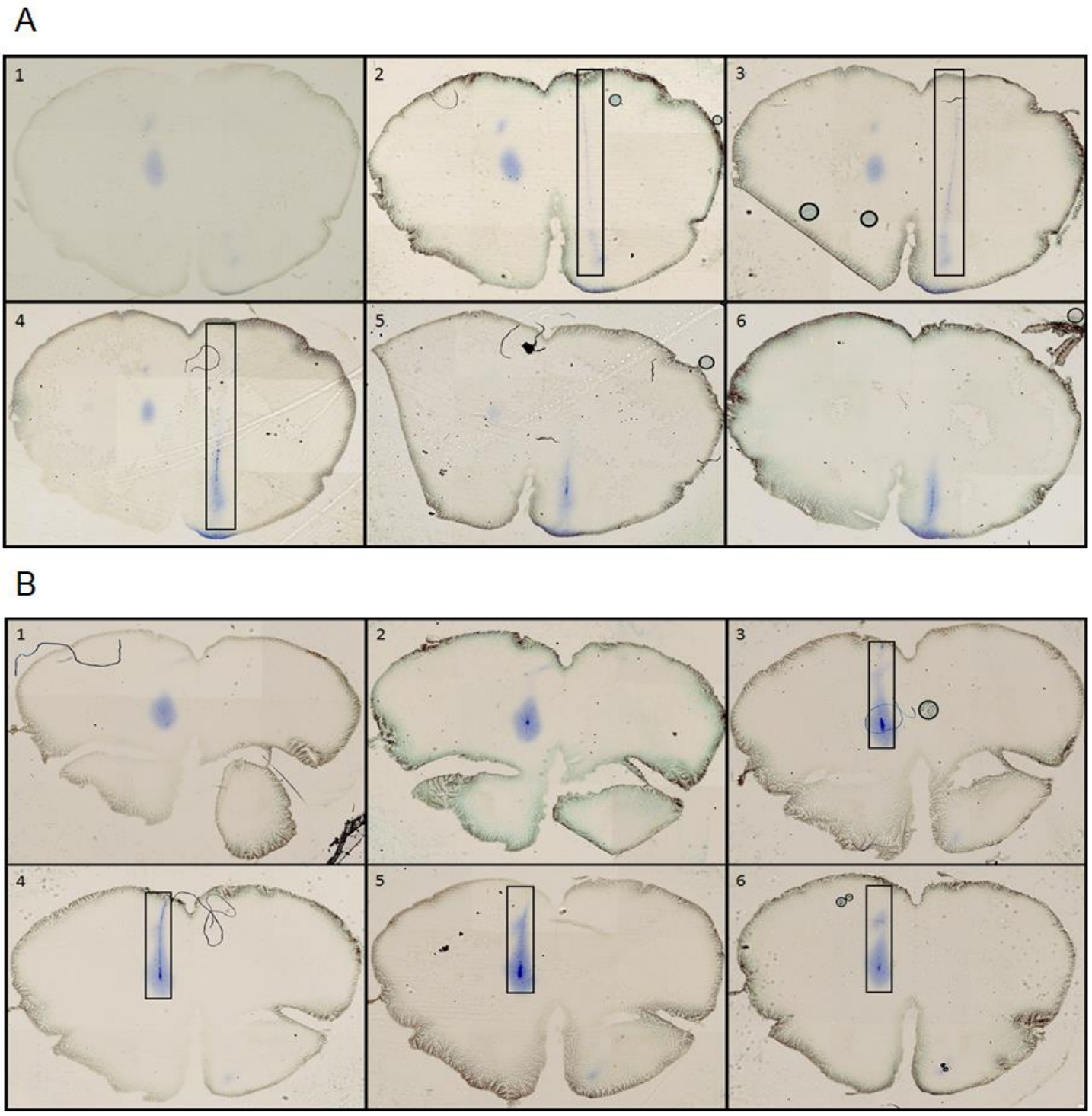

Figure 10 - Stereotaxic surgery with Evans Blue Injection at 10º of inclination. (A) Anterior to posterior brain slices from a mouse injected with Evans Blue into the NAcc **(B)** Anterior to posterior brain slices from a mouse injected with Evans Blue into the mPFC The black box indicates the current position of the glass micropipette tip during its descent until reaching its final DV coordinate. (n=3 animals)

In vivo electrophysiology

To first assess how these two specific brain regions are involved in social dominance behavior and if their intrinsic connectivity plays a role in this type of social behavior, we designed and implanted a MEA in both the mPFC and the NAcc. Furthermore, to get a finer resolution of what spectrum of specific behaviours possibly entails the establishment of a social dominance hierarchy, we divided the tube test into several different behavior epochs, as seen in **Figure 11.**

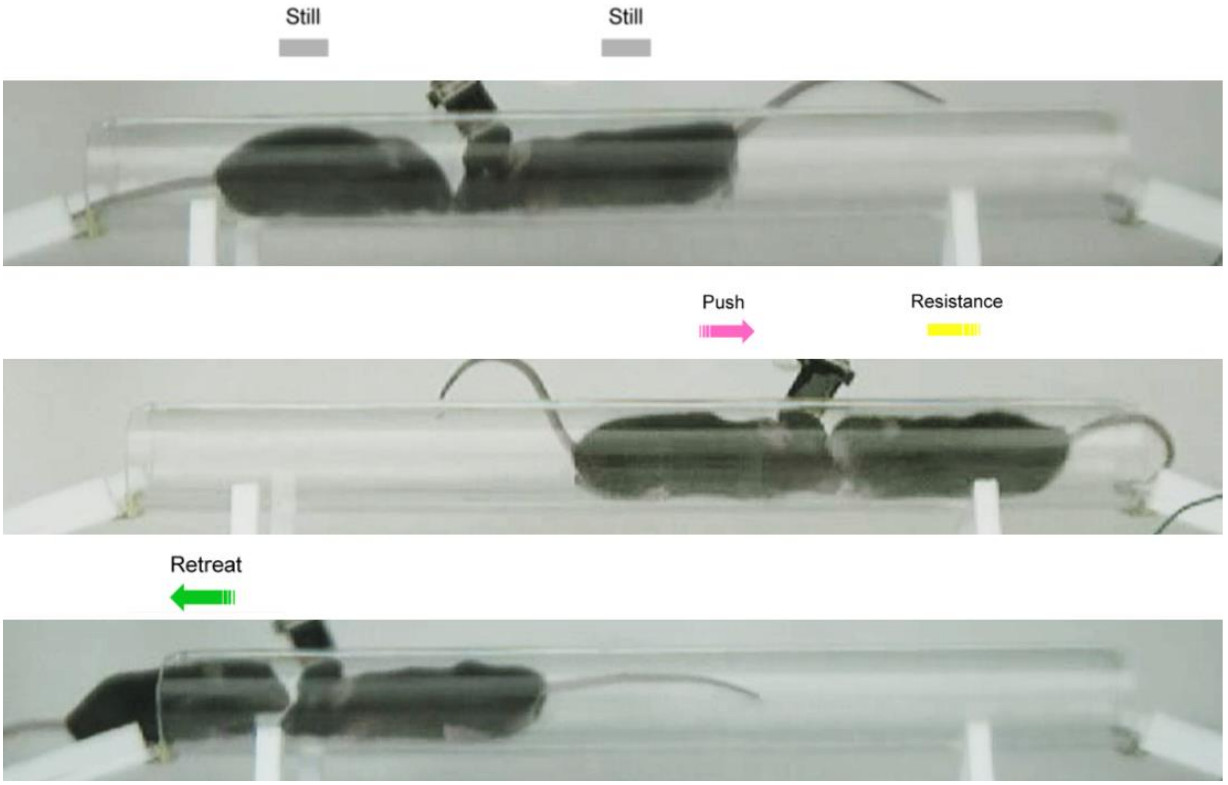

Figure 11. Characterization of tube test behavior. Schematic illustrating the different behavior epochs studied during tube test. Stillness: no movement except for sniffing (top); Push: one mouse shoves its head under another mouse (middle left); Resistance: hold on to territory when being pushed and the head is pushed up (middle right); Retreat: back out after being pushed or voluntarily withdraw (bottom).

Local Field Potentials

LFPs reflects the coordinated activity recorded in the extracellular space of the brain tissue. Traditional LFP analysis involves spectrograms and computing power spectra densities (PSDs) of these signals, capturing power at various frequencies in the signal in a specific time point. As such, we first analyzed this neural activity in several behavior epochs during the mouse´s trials on the habituation phase.

As we can observe in **Figure 12,** all the behaviors observed in the tube (walking, laying still and grooming) elicited a strong neuronal activity in the Theta band**,** in both the mPFC and NAcc. However, some specific behaviors showed differential peak activity in low frequencies within the two brain regions. For instance, laying still in the first section of the tube had its peak activity around 5Hz in both the mPFC and the NAcc **(Figure 12-B1)**. However, the peak activity in the mPFC was higher than in the NAcc. In contrast, laying still in the last section had a higher-powered peak of activity around 5Hz in the NAcc than in the mPFC **(Figure 12-B4)**. Furthermore, both when the mouse was grooming and when it left the tube, the peak activity was around 3Hz, although it was higher powered in the NAcc than in the mPFC.

When the mouse traveled the tube, we decided to analyze both halves of the tube to determine if there was any specific brain activity when in a particular area. Interestingly, we observed higher brain activity when the mouse was in the extremities of the tube than when in the middle, especially in the distal segment of the tube. **(Figure 12-A2/3).**

Next, we assessed the brain activity of these two brain regions when the mouse was confronted with an opponent within the tube. To do that, we analyzed the four different behavior epochs demonstrated in **Figure 11.**

Again, as can be seen by **Figure 13,** the same theta activity could be observed in all the studied behavior epochs. Interestingly, we observed the same pattern of activity in both brain regions when the mouse was in the last section of the tube **(Figure 12-3)** and when the opponent mouse retreated from the tube **(Figure 13-1).** However, analysis of the behavioral video indicated that the recorded mouse was in the middle section of the tube and not on the last section as previously observed. As such, this data suggests that this specific pattern may represent be a neuronal signature for “winning” a trial.

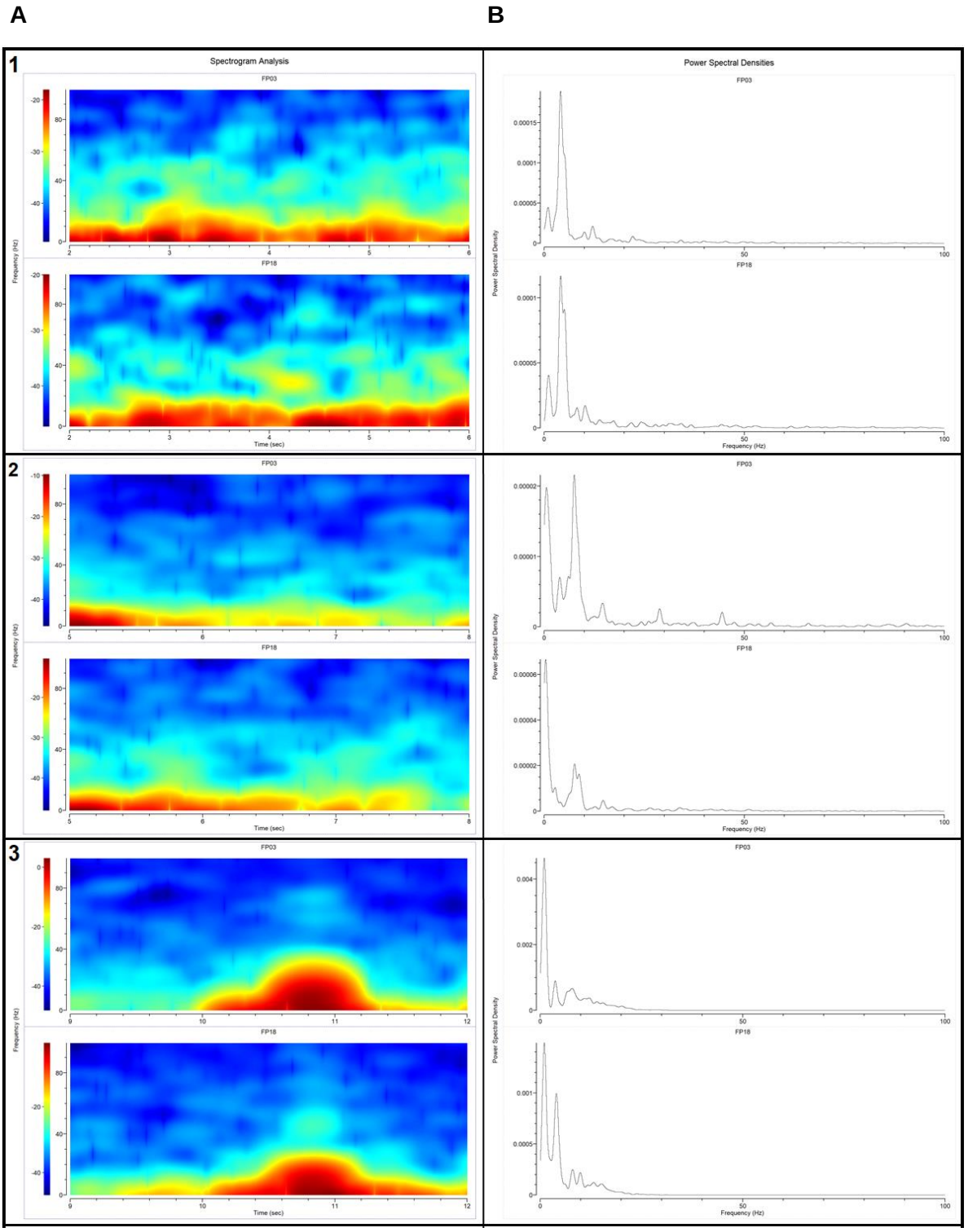

Figure 12. Different behavior epochs in the tube alone elicit neuronal activity in the Theta band (4-10Hz). (A) Two-dimensional plot of the spectrogram of the mouse´s movement in the tube. Time is on the x-axis; frequency is on the y-axis. Power is color-coded on a log scale of PSD (dB). FP03 (top) represents an electrode in the mPFC; FP18 (bottom) represents an electrode in the NAcc **(B) (B)** Two-dimensional plot of the LFP spectral power**;** frequency is on the y-axis. Power is provided in Raw Spectral Density. FP03 (top) represents an electrode in the mPFC; FP18 (bottom) represents an electrode in the NAcc. **(1)** Laying still in the first section of the tub**e (2)** Walking from the beginning until the first half of the tube **(3)** Walking from the middle until the end of the tube

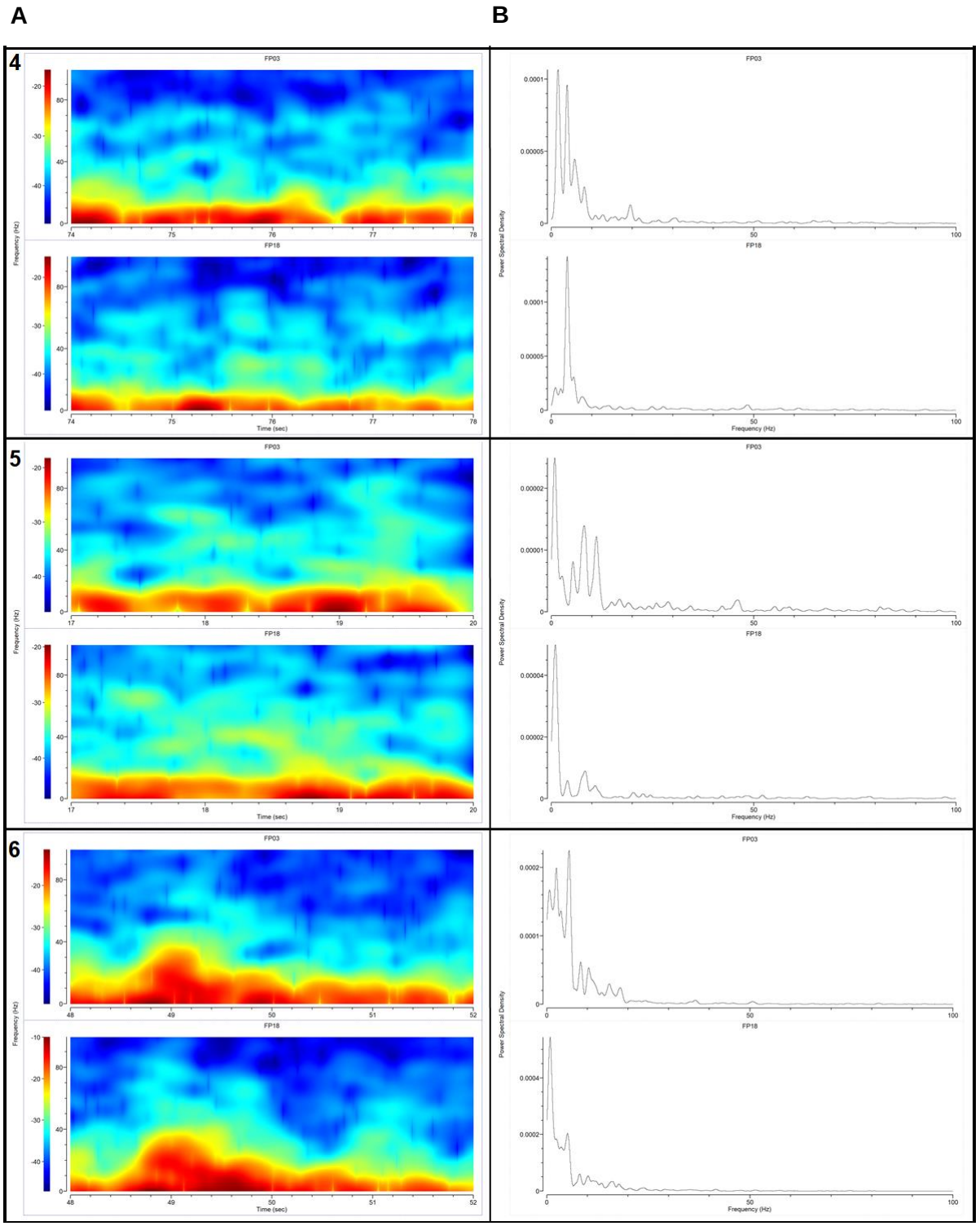

Figure 12 (cont). Different behavior epochs in the tube alone elicit neuronal activity in Theta band (4-10Hz). **(A)** Two-dimensional plot of the spectrogram of the mouse movement in the tube. Time is on the x-axis; frequency is on the y-axis. Power is color-coded on a log scale of PSD (dB). FP03 (top) represents an electrode in the mPFC; FP18 (bottom) represents an electrode in the NAcc **(B)** Two-dimensional plot of the LFP spectral power**;** frequency is on the y-axis. Power is provided in Raw Spectral Density. FP03 (top) represents an electrode in the mPFC; FP18 (bottom) represents an electrode in the NAcc. **(4**) Laying still in the last section **(5)** Mouse left the tube **(6) G**rooming

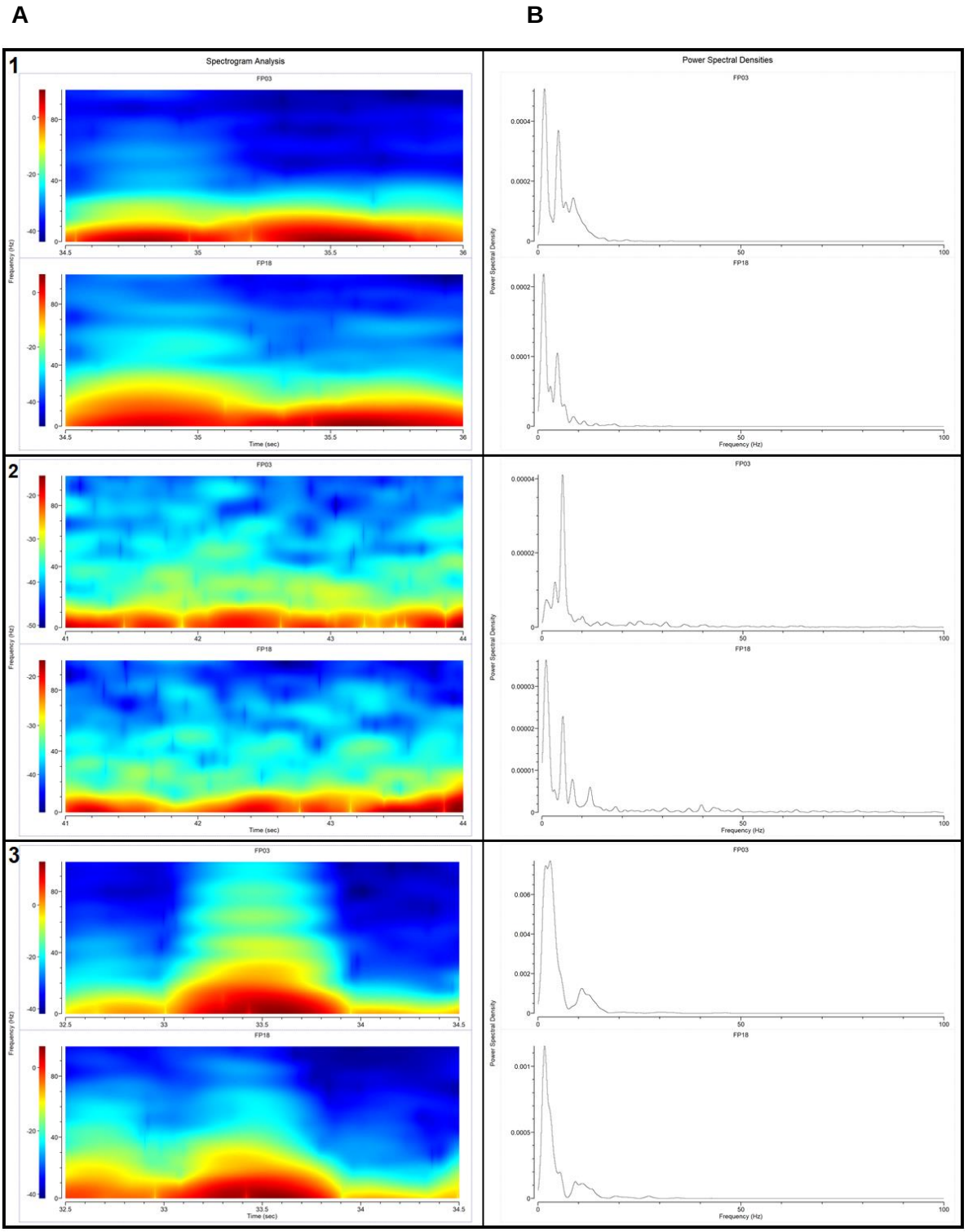

Figure 13. Different behavior epochs in the tube test elicit neuronal activity in the Theta band (4-10Hz). (A) Two-dimensional plot of the spectrogram of the mouse´s movement in the tube. Time is on the x-axis; frequency is on the y-axis. Power is color-coded on a log scale of PSD (dB). FP03 (top) represents an electrode in the mPFC; FP18 (bottom) represents an electrode in the NAcc **(B) (B)** Two-dimensional plot of the LFP spectral power**;** frequency is on the y-axis. Power is provided in Raw Spectral Density. FP03 (top) represents an electrode in the mPFC; FP18 (bottom) represents an electrode in the NAcc. **(1)** Recorded mouse pushes its opponent **(2)** Both mice are still **(3)** Recorded mouse is pushed and backs out

Optogenetic Trials

We also decided to use Optogenetics to determine if we could disrupt an already established dominance hierarchy by stimulating this corticostriatal projections in the tube test setting. To do that, first we delivered an AAV viral construct coding for ChR2 to the NAcc and implanted Optical Fibers in the mPFC, as described in the Methods section. As such, we designed an experimental timeline for our first set of optogenetic manipulation, as seen in **Figure 14.**

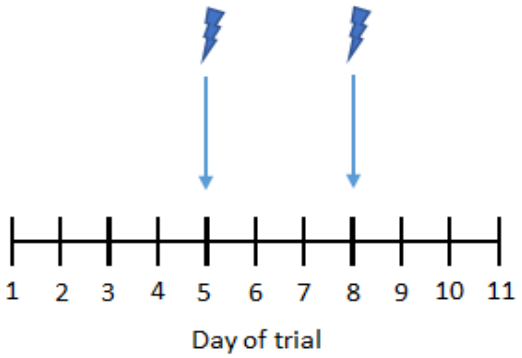

Figure 14– Experimental timeline for the first set of optogenetic trials. Timeline consisted of 11 days of trials. Photo stimulation was performed on day 5 and 8, as marked by the blue arrow. Each day consisted of 3 tube test trials except day 5 and day 8, where 9 trials were performed.

We first assessed the social ranks of each mouse of the pair being tested, based on the number of wins and losses in the tube test trial. As can be seen in **Figure 15 (A),** social ranks were well established and maintained during the first set of this experiment, before any photo stimulation occurred. Furthermore, the mean duration of each trial decreased along this segment timeline, indicating that the dominance hierarchy was strengthened by each day of the experiment **(Figure 15 (A)).**

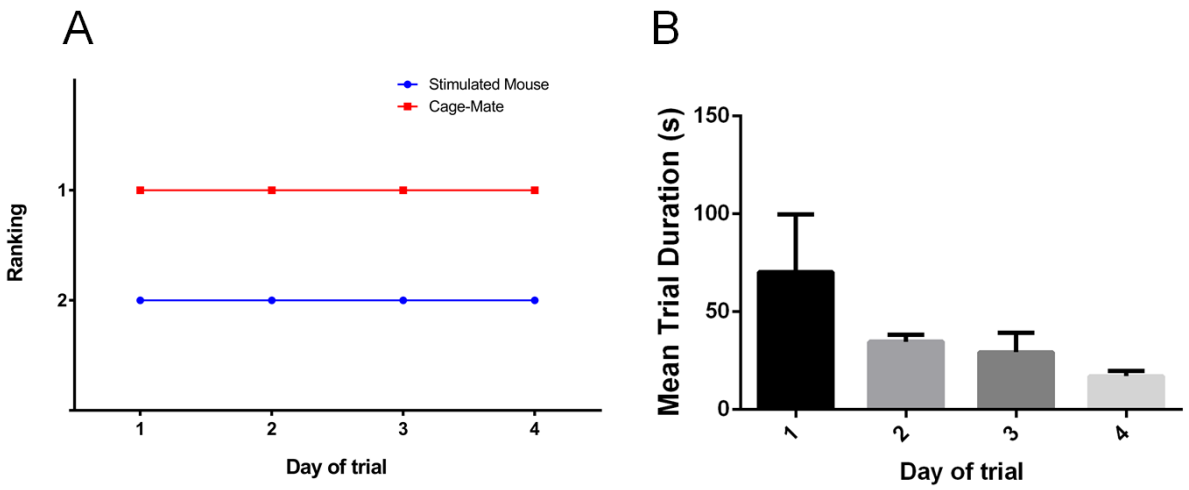

Figure 15 - Social rank was well established after 4 days of trials. (A) Social ranking was assigned based on the number of trial wins, with the stimulated mouse losing all the trials in each day (rank 2) and therefore, being considerate the subordinate one of the pair. **(B)** The mean duration of the trials, in seconds, decreased along time, indicating that a strong and well-established dominance hierarchy was in place.

We then tried to disrupt this dominance hierarchy by photo-stimulating the corticostriatal circuitry of the subordinate mouse. In the first two trials, photo stimulation was applied only when the subjects were touching their nose. However, as can be seen in **Figure 16 (A),** this stimulation was not sufficient to induce a change in rank. Interestingly, the duration of these trials was higher than when not stimulated (**Figure 16 (B)**). Furthermore, when we performed the next three trials without photo stimulation, the duration of the trials returned to the levels observed before. Based on this data, we hypothesized that our photo stimulation protocol was not strong enough to induce any noticeable alteration to the hierarchy. As such, we then performed three trials with active photo stimulation from the beginning until the end of the trial. Surprisingly, this alteration was enough to induce an alteration in the established social ranks, making the subordinate mouse win the three trials **(Figure 16 (A)).** Furthermore, the duration of the trials also increased**,** in comparison with both our previous photo stimulation protocol and when not photo-stimulated. **(Figure 16 (B)).** Moreover, the stimulated mouse also won the last trial of the day, even though no photo stimulation was applied. Moreover, the duration of the trial was lower than when photo-stimulated. Taken together, this suggests that the induced change could be permanent and that the observed increase in the trial duration is correlated to the optogenetic stimulation.

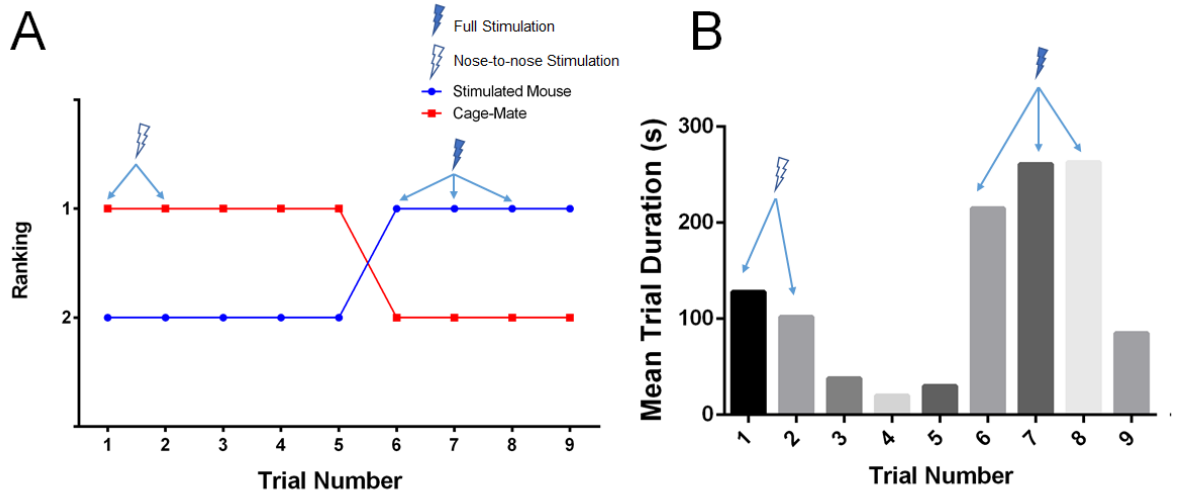

Figure 16 – Full, but not partial, photo stimulation induced a change in the established social ranks. (A) Discrete photo stimulation only when the subjects were touching their noses in the first 2 trials was not sufficient to induce a change in social rank (trials marked with arrows with a white lightning bolt). Trials without any marked arrow indicate that no photo stimulation was applied. Full stimulation from the beginning until the end of the trial was sufficient to induce a change in social ranks, with the subordinated mouse winning a trial for the first time (trials marked with arrows with a blue lightning bolt). **(B)** Duration of the trials increased in the trials were photo stimulation was applied. (trials marked with arrows)

We then assessed if the observed change in rank was still present in the days that followed. As can be seen in **Figure 17,** the stimulated mouse remained the dominant of the pair, even without any photo stimulation applied. However, the mean trial duration was higher than the previous day (**Figure 16),** possibly suggesting that the previous dominant mouse was trying to regain the top rank, resulting in longer trials.

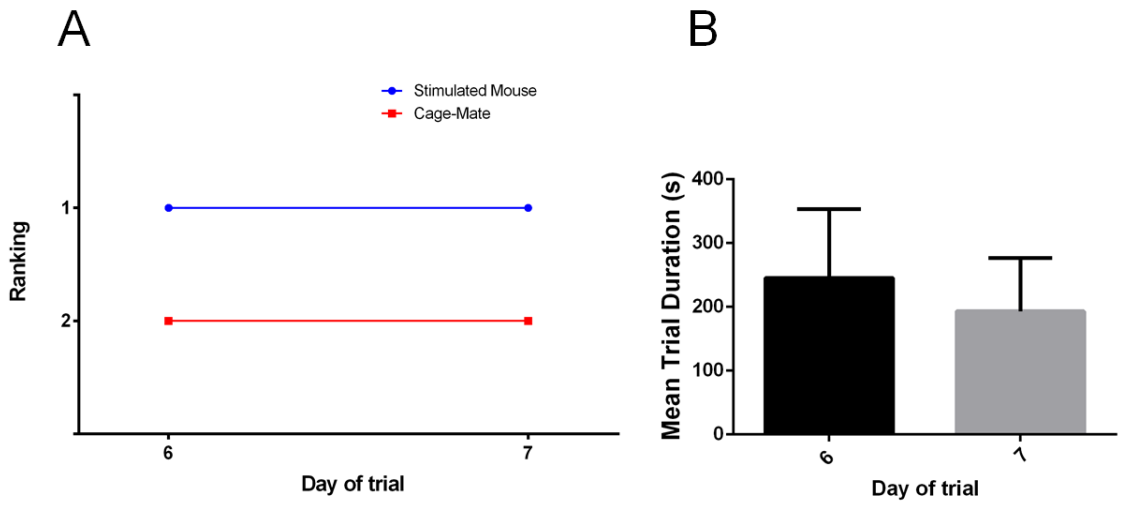

Figure 17 – The observed change in social ranking remained even with no photo stimulation applied. (A) The previous subordinate mouse now became the dominant one, even when no photo stimulation was delivered.

(B) The mean duration of the trials, in seconds, was considerably higher than previous trials, possibly indicating that the previously dominant mouse was trying to regain its social rank.

Interestingly, in the second day of photo stimulation (day 8 of the experimental timeline), an erratic dominance hierarchy could be observed, with the stimulated mouse winning and losing trials in alternation **(Figure 18 (A))**. Furthermore, trial duration was also erratic **(Figure 18 (B)),** suggesting that the currently disrupted hierarchy was returning to the previous established one. As such, full photo stimulation was applied on trials five through seven to strengthen the current hierarchy. Only the third episode resulted in a win, again showing an increase in trial duration. When no stimulation was applied, trial duration reverted to average trial duration.

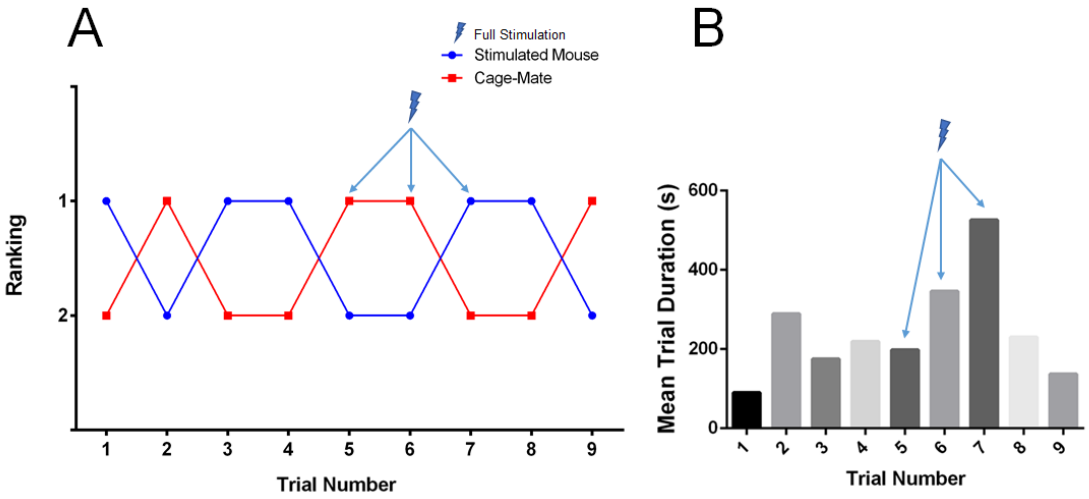

Figure 18 – Second round of photo stimulation resulted in random trial outcomes. (A) The stimulated mouse appeared to both win and lose trials without an observable pattern (trials without any marked arrow). Full stimulation was not sufficient to induce a change in social ranks, resulting in random trial outcomes, with the subordinated mouse losing the first 2 photo-stimulated trials and winning the third (trials marked with arrows with a blue lightning bolt). The last 2 trials also appeared to have random outcomes. **(B)** Duration of the trials also appeared to be random, with photo-stimulated trials being the longest ones. (trials marked with arrows)

Furthermore, on the last three days of our experimental timeline, we observed the previously disrupted hierarchy re-structuring **(Figure 19 (A)),** suggesting that the second set of photo stimulation trials failed to strengthen the new dominance rankings.

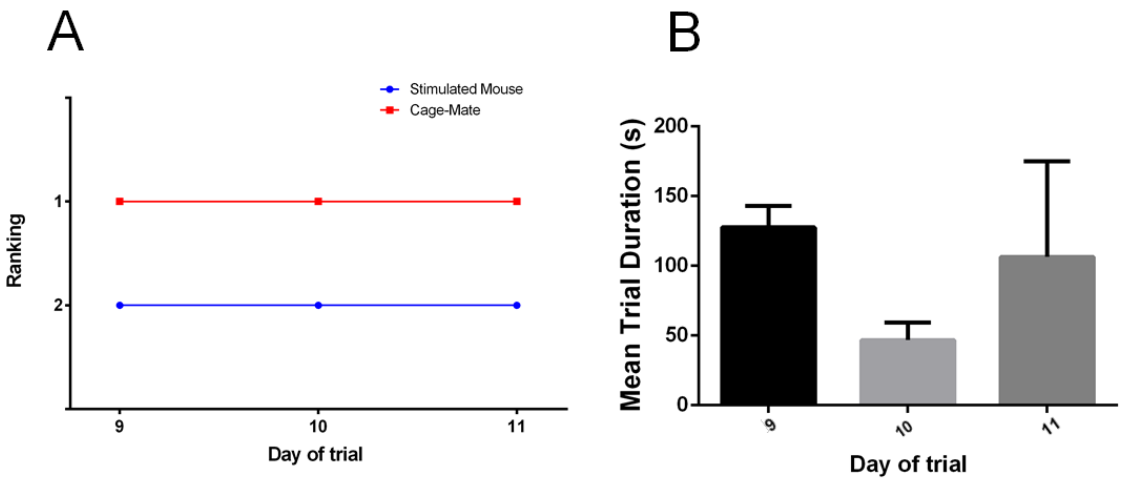

Figure 19 – **The previously disrupted hierarchy was now taken over by the first established hierarchy. (A)** The stimulated mouse returned to its initial social rank and vice versa. **(B)** Duration of the trials was once again random.

Unfortunately, the stimulated mouse died of unknown causes on the day after the last day of trials. This could mean that the erratic behavior seen in the second set of photo stimulations could have arisen from an animal intrinsic problem and not from the photo stimulation *per se.*

Second Set of Optogenetic Trials

Our second set of optogenetic trials had a few key experimental setup alterations from the previous setup, along with new experimental timeline, as described in **Figure 20**. First the photo stimulation was given unilaterally. Second, the trials on days two to five were performed with the coupler fiber connected to both the subjects, to determine if the apparatus itself impacted the outcome and/or the duration of the trials. Third, each photo stimulation days consisted of 3 tube test trials instead of the 9 from the first set of optogenetic trials. Lastly, due to a technical problem with the laser-splitter, the photo stimulation power was reduced in half in comparison with the first set.

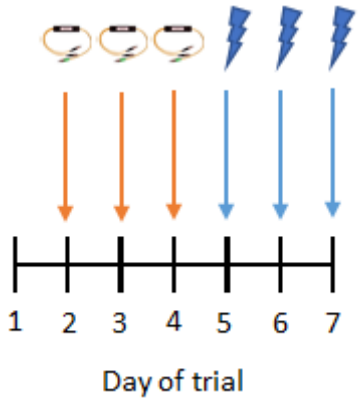

Figure 20 – Experimental timeline for the second set of optogenetic trials. Timeline consisted of 7 days of trials. Trials on day 2 through 4 were performed with the coupler fiber connected, as marked by the orange arrow. Photo stimulation was performed on day 5 through 7, as marked by the blue arrow. Each day consisted of 3 tube test trials.

The first 4 days of trials provided with the exact same results as our first set of optogenetic trials, with a clear and well-established dominance hierarchy (**Figure 21).** Furthermore, the duration of the trials remained stable across the four days, meaning that the coupler fiber apparatus had a negligible effect on the trial.

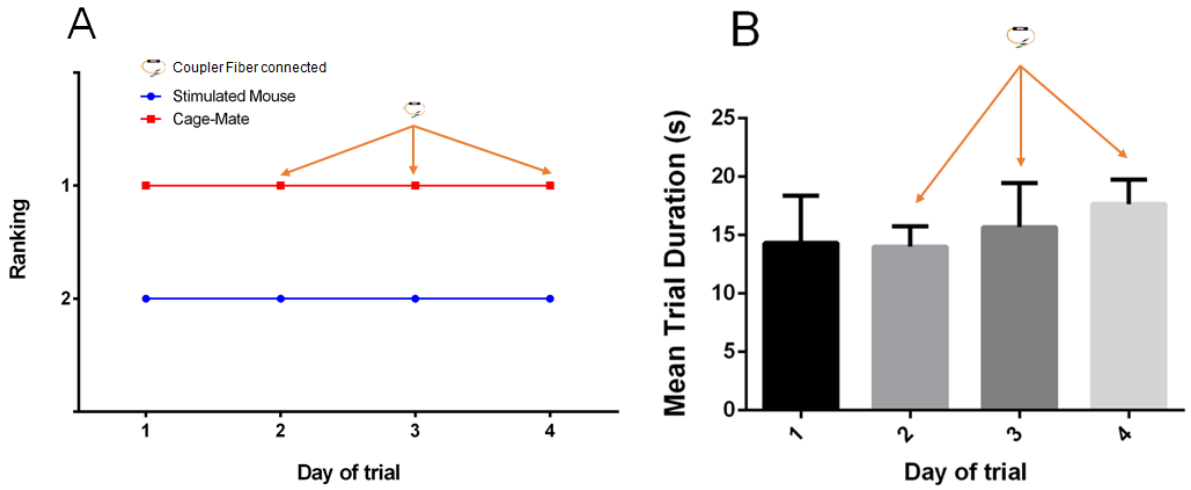

Figure 21 - Social rank was well established after 4 days of trials. (A) Social ranking was assigned based on the number of trial wins, with the stimulated mouse losing all the trials in each day and therefore, being considerate the subordinate one of the pair. Trials on days 2 to 4 were performed with coupler fiber connected to both the subjects but did not change the outcome of the battles **(B)** The mean duration of the trials, in seconds, was maintained along the 4 days, indicating that a strong and well-established dominance hierarchy was in place. The connection to the coupler fiber also had a negligible effect on the trials duration

However, we saw no changes in the established social ranks, even after three days of photo stimulation. Furthermore, the duration of the trials remained the same throughout these days (**Figure 22 (A/B)).** This negative result may be explained from the fact that a unilateral photo stimulation was

insufficient to elicit a significant change in the hierarchy. Coupled with the fact that the stimulation power was half of the one in our first set of optogenetic trials, as such, one possibility is that not enough cells were being stimulated to produce a behavioral effect.

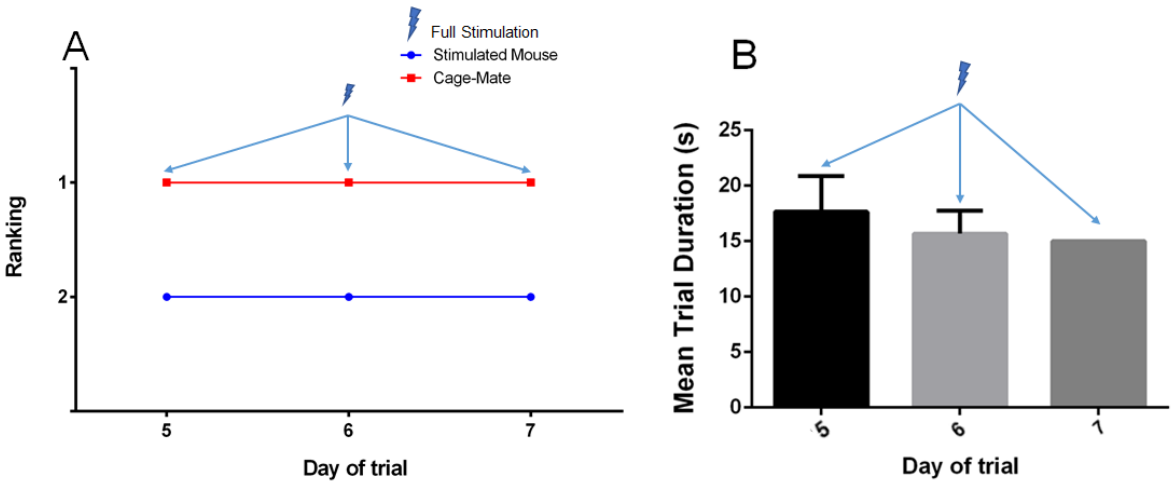

Figure 22 – Unilateral photo stimulation was not sufficient to induce changes in social rankings. (A) Unilateral stimulation was not sufficient to induce a change in social ranks, with the stimulated mouse losing all the trials in the 3 photo-stimulated days (trials marked with arrows). **(B)** Duration of the trials did not appear to be affect by the photo stimulation procedure (trials marked with arrows).

Fluorescence Imaging Results

Our first set of optogenetic trials was performed according to the "0 degrees" Approach, in both the placement of the glass micropipette and the Optical Fiber implantation.

As can be seen **Figure 23 (B),** the NAcc was successfully reached, with a good level of infection. Furthermore, we could also see infected cells in the mPFC, mainly in the InfraLimbic area **(Figure 23 (A)),** meaning that we successfully reached the corticostriatal projections. However, the optical fiber implant, marked by the white arrow in **Figure 23 (A)**, appeared to be slightly shifted to the intend mark, but the target region falls within the stimulation light cone.

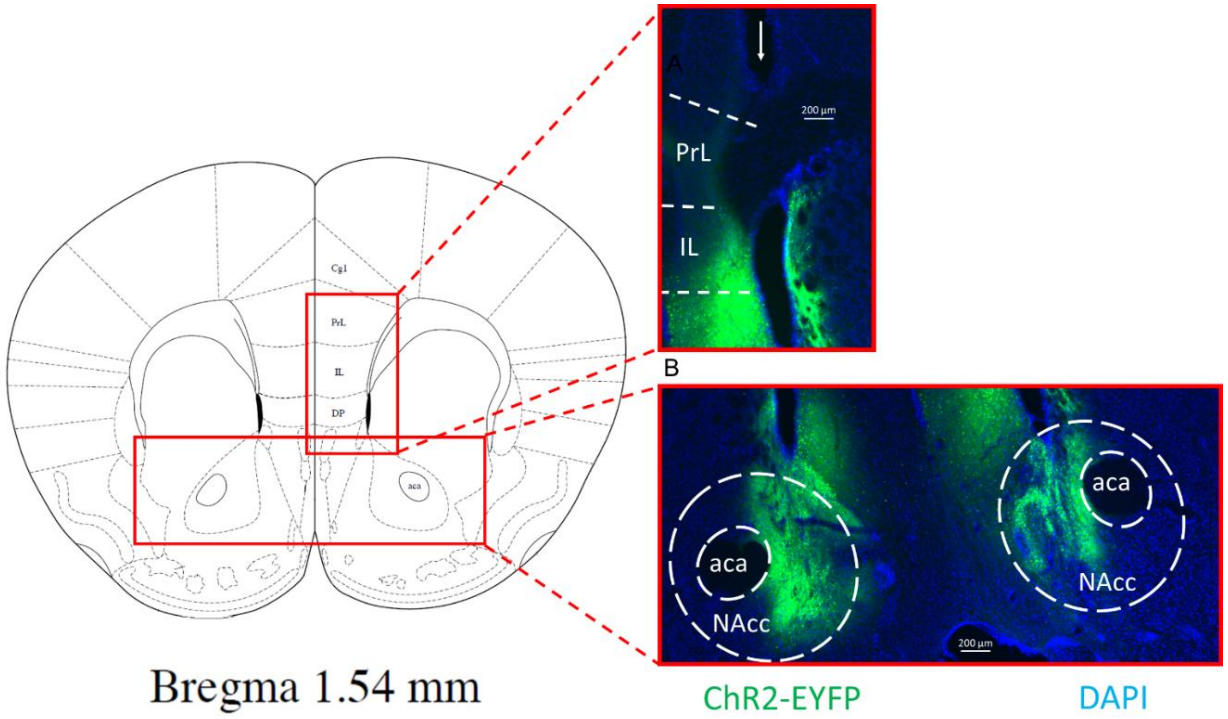

Figure 23 - Viral injection using the "0 degrees" Approach successfully infected corticostriatal projections. **(A)** Infected regions of the mPFC, with the IL being the most infected region. Optical Fiber placement is indicated by the white arrow. Scale bar, 200 um **(B)** Viral infection ranged from the NAcc to the NAc shell. Scale bar, 200 µm

Our second set of optogenetic trials was done according using "10 degrees" Approach, in both the placement of the glass micropipette and the Optical Fiber implantation.

Again, as can be seen **Figure 24 (A)**, the the NAcc was successfully targeted, with a good level of infection. However, in comparison to **Figure 23,** we could clearly see that the infection was more widespread, reaching outside of the NAcc into the Nucleus Accumbens shell. Furthermore, more areas of the mPFC, including the PrL and the Cg1, were infected (**Figure 24 (B))**

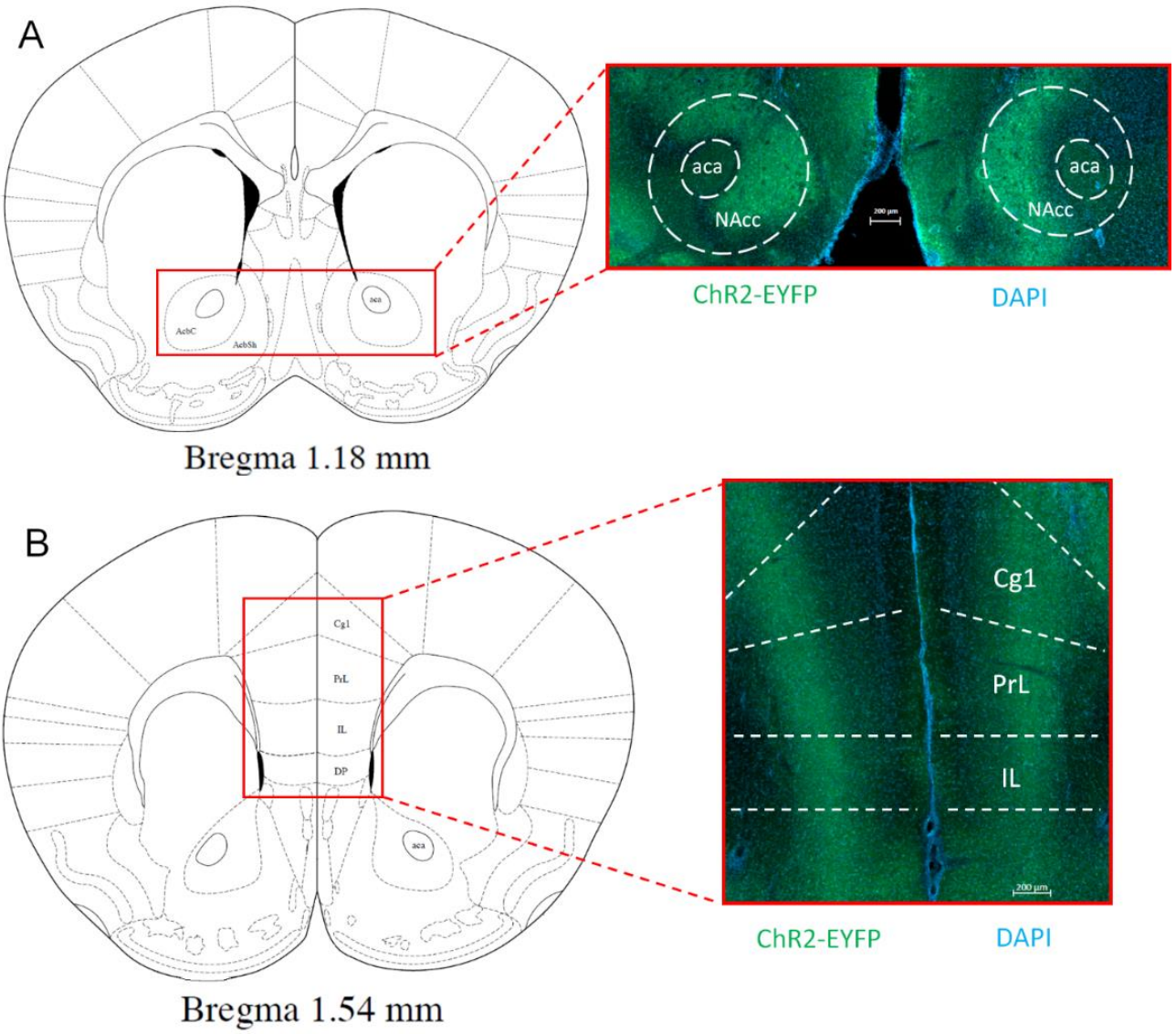

Figure 24 - Viral injection using the "10 degrees" Approach successfully infected corticostriatal projections. (A) Infected regions of the mPFC, with the Cg1, PrL and the IL having a good level of viral infection. Scale bar, 200 um **(B)** Viral infection ranged from the NAcc to the NAc shell. Scale bar, 200 µm

cFos expression

To determine if the photo stimulation protocol used in our first set of optogenetic trials corresponded directly to neural activation, we tried to quantify the immediate early gene cFos expression. As can be seen in **Figure 25**, we used unilateral photo-stimulated, indicated by the white arrow and we could see cFos positive cells in both hemispheres, suggesting there is ipsilateral and contralateral activation when photo-stimulation is performed.

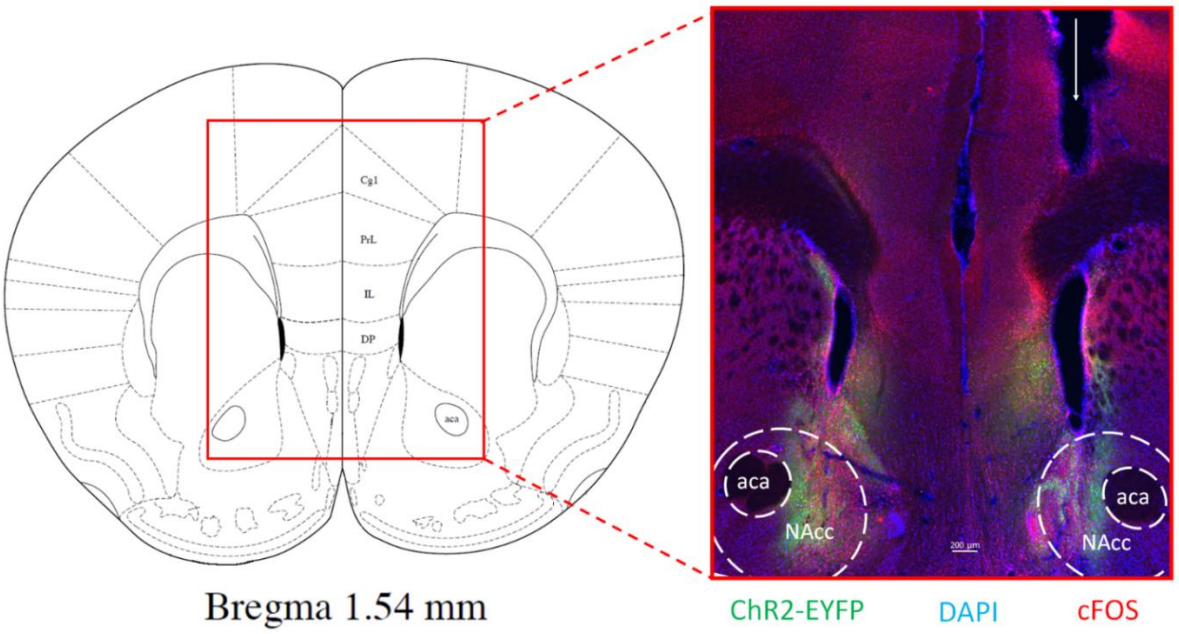

Figure 25 - c-Fos expression induced by photo stimulation. Fiber optic implant marked by the white arrow. Scale bar, 200 µm

Chapter IV | Discussion

Animals in a social group interact and establish dominance relationships that culminate in social stratification and the formation of a hierarchy. This process is initially characterized by frequent agonistic encounters where dominance across individuals is not clearly defined. Eventually stability is reached, dominance relations become well defined, and aggressive encounters decrease in frequency. However, little is known about what neuronal circuits responsible for the emergence and establishment of this social behavior. As mentioned previously, imaging studies performed in humans, such as the ones by Chiao et al (2010)[31] and Zink et al (2008)[32], suggest that the mPFC and the NAcc are significantly active during social hierarchy behavior. Furthermore, studies done in mice, such as the ones by the Hu lab[25,50], Felix-Ortiz et al (2016)[55] and Amadei et al (2017)[89], further confirm their role in social behavior. However, none of the above studies analyzed the intrinsic connectivity between these two regions and its role in the formation and establishment of a dominance hierarchy. As such, we set the main goal with this project to optimize the experimental procedures to probe this question.

As both observation and perturbation studies are needed for further increasing our understanding of brain function, we divided our focus into two main areas: functionally understanding what is happening within these brains regions during this social behavior; and modulating the activity of these projections to disrupt an already established hierarchy. Both tasks are highly complex to execute, requiring the mastering of advanced techniques and tools. As can be expected, such cannot come without its obstacles, as discussed below.

One of these tool is the stereotaxic surgery, invaluable for the study of systems neuroscience, with applications ranging from the injection of anatomical tracers and viral constructs to the implantation of electrodes [91]. In fact, this technique is the cornerstone for all the other tools used in this project and as such, correct implementation was of the uttermost importance.

The set of stereotaxic coordinates used in this project were acquired from “The Mouse Brain in Stereotaxic Coordinates”[92] atlas from George Paxinos, given in three-dimensional distances from the bregma (in mm). This specific bregma coordinate represents the intersection of the coronal and sagittal sutures on the surface of the skull and can vary from mouse to mouse. As it is the cornerstone for all the other coordinates, a incorrect bregma locations can lead to a targeting of wrong brain region. As it is highly variable, our method of setting this coordinate correctly relied on drawing imaginary lines from the sutures and considering the bregma as the intersection point of these lines the bregma, instead of the physical intersection point.

Once again, as this is an advanced technique, we performed a first set of stereotaxic surgeries where we injected Evans Blue in to the mPFC and the NAcc of the mouse (**Figure 9).** Although the target areas were reached, we could not see a clear single straight trace of dye in any slice observed. This "needle trace" marker is our internal control that indicates that the glass micropipette descent was perpendicular to the brain surface. The lack thereof of this "needle trace" indicated that this descent was tilted, possibly due to a stereotaxic apparatus not properly set up, an incorrectly placed animal during the procedure or a technical error during the slicing of the brain for imaging. This represented the first obstacle to our work since a tilted injection into the brain compromises the populations being target and induces a significant caudal shift in more ventral locations. Since our goal is to target both the mPFC and the ventral striatum simultaneously, a correct insertion is critical.

After all causes mentioned above were ruled out, we began to question if the brain itself was tilted relative to the skull surface, which could explain the recurrence of this observation. After searching in the literature, we encountered the work of Charles W. Morgan et al (2014)[93], indicating there is indeed a 15° slant of the skull relative to the brain is often present in C57 strain **(Supplementary Figure 5)**. After additional calculations based on our own data, we postulated the slant to be closer to 10-12° degrees instead of the 15°.

To address this possibility, we performed another set of stereotaxic surgeries where we injected Evans Blue in to the mPFC and the NAcc of the mouse with a 10° descent angle, as described in **Supplementary Figure 3 (B).** As can be seen in **Figure 10,** the "needle trace" was now clearly visible, suggesting that the micropipette descent was now perpendicular to the brain surface.

Moving to our first main goal, one technique that allows us to measure brain activity in real-time during awake behavior is *in vivo* electrophysiology. By implanting electrodes into the mPFC and the NAcc, we can better comprehend how these two regions "communicate" with each other in specific social behavior epochs, further expanding our knowledge of their intrinsic connectivity.

The build material of the electrode used is important for the recording quality. Tungsten, the material of which our MEA is made is the most commonly used material because of its stiffness, biocompatibility and cost. Furthermore, the shape of the electrodes is also specifically designed for the experiment in question. A recording electrode that is optimized for single unit isolation normally has a small exposed metal area and a high electrode impedance whereas a recording electrode optimized for field potentials has a higher exposed area with a lower impedance.

These electrodes record the signal in the brain extracellular medium which is a superposition signal of LFPs and spike activity, being these the two primary measurements: Spikes are the recorded activity of an individual neuron while local field potential activity is generated by extracellular currents due to synchronized activity in a local population of cells, with a temporal structure mainly in the frequency range of 0-100 Hz[94]. Normally, the LFP signal has a larger amplitude than action potentials and by low pass filtering, it we are able to separate it from the spike activity.

This LFP activity is of critical importance as it captures important integrative synaptic processes that otherwise would not be measured by the spiking activity of a few neurons[95]. Furthermore, several studies recurred to LFPs to investigate how specific cortical network mechanisms relate to concrete behavior traits, ranging from sensory processing [96–98], motor planning [99,100], to higher cognitive processes [101,102]

Traditional LFP analysis revolve around decomposing and interpreting this data in the frequency domain. Spectrograms and power spectra densities (PSDs) of these signals can capture power at various frequencies in the signal in a specific time point.

We found that all the observed behaviors, both when alone and when in a confrontation setting, had their peak neuronal activity at the Theta band (4-10Hz). This frequencies have been previously shown to be involved in the amygdalohippocampal circuit rhythm synchronization during fear memory retrieval [103,104].

Of great interest, we observed that a specific pattern within this band could be observed when the animal was at the last section of the tube **(Figure 12-3)** and when its opponent retreated from the tube **(Figure 13-1).** This suggests that a specific brain pattern activity may be responsible for signaling or encoding the neuronal correlates of a dominance encounter victory.

Although this data indicates that these regions are in fact involved in social dominance behavior, further analysis are required to fully determine that their intrinsic connection is the one responsible for the data observed. Analysis such as the Spike–field coherence, where we measure how single and multiunit spikes interact with local field potentials, must be performed.

The last focus of this project was to try and modulate the activity of these projections to disrupt an already established hierarchy. To do this, two techniques present clear potential, chemogenetics and optogenetics. However, we required a tool that would allow us to activate these

projections with high spatial and temporal precision. As such, we choose optogenetics as the technique to modulate the activity of these projections.

This fairly recent technology fundamentally consists of genetically encoding light-gated microbial opsins, which can be ion channels, pumps or receptors, to the membrane of neurons to then be manipulated through controlled illumination protocols at the transduced tissue. Our chosen opsin ChR2(H134R) is a cation channel with its peak activation at 470nm and with Off Kinetics of 18 ms. When photo-stimulated with blue-light, inward currents of cations lead to a depolarization of the neuronal membrane potential, positively modulating the firing of action potentials. The most common optogenetic *in vivo* protocols rely on the stereotactic delivery of genetically modified viruses carrying the opsin gene. Viral expression systems offer several advantages as they offer a versatile application and high infectivity rate. The most commonly used viruses are the lenti and adeno-associated (AAV) viruses, which have already been described as vectors in optogenetic studies conducted in mouse, rat and primates [105]. This technology is of interest as can be used to target entire projections of neurons, as demonstrated by Felix-Ortiz et al[55] and Amadei et al[89]. Furthermore, as the opsin gene products are efficient in membrane trafficking and that light is projected to the axons of the transduced neurons and not to the soma, this technique allows for the recruitment of neurons along their wiring pattern rather than their genetic information [106–109].

With our strategy of injecting the viral vector containing the ChR2 construct in the NAcc, but only stimulating in the mPFC, we made sure that only these corticostriatal projections were being stimulated, as seen in **Figure 5.** Each set of Optogenetic Trials consisted of four mice injected with ChR2 and implanted with Optical Fibers, corresponding to a cage each. However, only two mice per set survived: two animals died during surgery, one during the recovery process and one a week after the surgery procedure of unknown causes. A third set of Optogenetic Trials was underway with two animals injected, but one removed the dental cement along with the fibers, invalidating the continuity of this set of trials. This recurring problem, along with the low number of animals surviving the surgeries (~50%), constituted one of the main challenges encountered during this thesis. A fourth set of optogenetic trials are now underway with eight animals (two cages) with a survival rate of 100%. We are also testing a new optimization where we add glue to the Optical Fibers and implant 2 stainless steel screws to better anchor the cement/ferrule mixture to the skull.

In our first set of Optogenetic Trials, we first assessed the social ranks of each mouse of the pair by running 4 days of trials, with 3 trials each. First, the test subjects need to interact to establish relations of dominance and crystalize their position in the hierarchy. As can be seen in **Figure 15 (A)**,

the social ranks between the pair were well established, with the subordinate consistently losing and the dominant consistently winning. As the cage tested only had these two mice, the hierarchy was well-consolidated and with less room for changes in comparison with cages with more mice. Furthermore, the duration of the trials decreased along those four days (**Figure 15 (B)**. This larger trial duration is expected during the first few trials most likely due to the habituation to the tube setting and establish dominance relationships in this context. Afterwards, once the hierarchy is firmly settled, the main process in tube test dyads would be the perception on the social ranking of the opponent.

We first hypothesized that activating this circuitry would increase the subordinate mouse aggressiveness and stimulate a signal "reward". Furthermore, communication of social hierarchy in rats, was described to be a process that occurs through sniffing pattern during face-to-face interactions[110]. As such, an interesting behavior epoch to stimulate would be when the animals were touching their noses. However, as can be seen in **Figure 16 (A)**, this partial stimulation was not enough to induce any observable change in social ranks. However, the duration of trials was higher than the previous days, as seen in **Figure 16 (B)**. One possibility is that this could be due to the stimulated mouse resisting more against the pushes of the dominant mouse.

Based in these results, we decided to deliver photo-stimulation from the beginning until the end of the trial. Surprisingly, this stimulation protocol was enough to induce a change in the established social ranks, with the subordinate now winning the trials **(Figure 16 (A))**. However, the battles were almost four times longer in comparison when not photo-stimulated **(Figure 16 (B))**.

Interestingly, even though no photo stimulation was delivered, the subordinated mouse won the last trial of that day and the consequent 2 days of trials **(Figure 17 (A))**. This may suggest the presence of a "winner effect", where animals increase their probability of victory after winning previous trials [33,50,111,112]. This effect may be mediated by long-lasting synaptic strengthening of these corticostriatal projections after repeated winning. If this is the case, we should be able to detect enhanced synaptic strength in the mPFC – NAcc circuit after repeated winning. One way to test this hypothesis is to inject a viral construct coding for ChR2 in the mPFC and then record light-evoked field responses in the mPFC-NAcc axonal terminals using an optrode. Accordingly, a possible experimental design would be to measure the field responses in a normal condition to get baseline levels, followed by photo-stimulation of these projections and, if a change in social rank was observed, measure the field responses in these terminals in the following days of trials with no photo-stimulation applied. Furthermore, we could also hypothetically interrupt this sustained winning by reversing the synaptic strengthening in the mPFC - NAcc circuit. As such, we could use an optical LTD protocol, such as low-

frequency stimulation [113,114], at these axon terminals after a number of stimulated wins and see if the "winning streak" came to an halt.

On the second day of photo stimulation, the outcomes of the trials appeared to be random, with the subordinate mouse both winning and losing battles **(Figure 18 (A))**. This suggested that, somehow, the first established hierarchy was taking over the disrupted one. As such, we photo-stimulated the subordinate mouse to determine if we could secure the current hierarchy. Intriguingly, even when stimulated, the outcomes of the battles continued to be variable, although slightly longer than before **(Figure 18 (B))**.

Although not targeting a specific set of projections, a recent study done by the Hu lab[50] found that a unilateral, 100Hz phasic photo stimulation to the subordinate mouse dmPFC was enough to elicit an upward change in social rank. As this region highly projects to the NAcc, their results strengthen the hypothesis of a key role played by corticostriatal projections in social dominance behavior.

As such, and although their results were from a cage with four mice, with more social ranks available and as such, a not so rigid hierarchy, and frequency modulated photo stimulation, we decided to test if a unilateral photo stimulation protocol was enough to induce the same observed change in social ranks for our second set of Optogenetic Trials. In this set we also tried to determine if the coupler fiber apparatus itself had any effect on the trial's outcome and duration, as seen in **Figure 20.**

As can be observed in **Figure 21,** the coupler fiber connected had a negligible effect on both the outcome and the duration of the battles. Furthermore, the social hierarchy was well established, with the subordinate mouse losing and the dominant winning all the trials.

However, contrary to what was described by other groups, we could not induce any change in social rank with a unilateral photo stimulation protocol **(Figure 22 (A))**. Furthermore, the durations of the battles remained the same throughout the photo stimulation days **(Figure 22 (B))**. This negative result can be ascribed to several reasons:

First, our photo stimulation protocol was non-frequency modulated, contrary to the 100HZ stimulation. Depending on the cell type and the region stimulated (axon vs soma) as well as the brain region of interest and light stimulus intensity, the latency to induce light-evoked spikes and the precision of evoked spike timing may vary.[115,116]. For instance, Gradinaru et al (2009)[106] demonstrated

that high-frequency stimulation of the afferent fibres to the STN greatly silenced the structure whereas low-frequency stimulation increased its activity. Furthermore, Nabavi et al demonstrated that low-frequency and high-frequency stimulation could serve as an optical LTD and LTP protocol, respectively[113]. As such, future *in vitro* Ephys experiments, using brain slices injected with ChR2, are required to correctly determine the best photo-stimulation protocol.

Second, the optogenetic results from Hu´s lab were from a different approach used in comparison with our own. By injecting the viral construct coding for ChR2 in the mPFC and stimulating in the same injection site [50], they were not activating a specific set of projections, but rather all of the circuits the mPFC and mPFC afferents. As such, a unilateral stimulation could result in a greater net effect than when only a set of projections are activated. As such, and given the precise nature of our approach, a unilateral stimulation may not be enough to elicit any change in rank.

Furthermore, this unilateral photo stimulation, due to a technical problem with our laser splitter, was delivered with half the power in comparison with our first set of trials. As it was previously shown in the literature, the laser intensity required for the subordinate mouse to win correlated with the rank distance that the mouse needed to move, indicating a dosage-dependent relationship[50]. Therefore, the reduced laser power that was delivered in this set of trials may have not been enough to disrupt the established social ranks. This raises the interesting question if different power levels of photo stimulation in different behavior epochs could result in a better manipulation of a dominance hierarchy. As such, further trials, with different power levels applied, are required to completely understand how this relationship works with these corticostriatal projections

Lastly, this negative result may have also been explained by more technical issues, such as misplacement of the Optical Fibers and/or a low level of infection. As we were unable to process the stimulated mouse from this set of trials, these questions remain unanswered here.

To determine the levels of infection achieved, as well as the placement of the optical fibers, we processed the mouse´s brain for immunofluorescence imaging. As mentioned previously, our first set of optogenetic trials was done according to the “0 degrees” Approach, in both the placement of the glass micropipette and the Optical Fiber implantation. As can be seen **Figure 23 (B),** the NAcc was successfully reached, with a good level of infection. Furthermore, we could also see infected cells in the mPFC, mainly in the Infralimbic area **(Figure 23 (A)),** meaning that we successfully reached the corticostriatal projections. However, we could only see a low number of marked cells in the PrL. As both these regions highly innervate the NAcc [81] **(Figure 8**), the lack of more marked cells in the PrL

could be due to a lower amount of virus being delivered to the NAcc, or that the normal amount was delivered but had a lower infection rate. Furthermore, our injection sites could also have hit only the subregions of the NAcc innervated by the IL projections, resulting in low number of neurons transfected in other regions of the mPFC. In addition, the optical fiber implant, marked by the white arrow in **Figure 23 (A)**, appeared to be slightly leftward to the intend mark. This error could not be mitigated by our current approach of implantation as we could not place the optical fibers further inward, as that they would clash, rendering impossible the connection with the coupler fiber. As such, for the second set of optogenetic trials, we updated our Optical Fiber Implantation angle from 0° to 10° on a dorso-lateral axis. (**Supplementary Figure 4 (B)).**

As such, our second set of optogenetic trials was done according using "10 degrees" Approach, in both the placement of the glass micropipette and the Optical Fiber implantation.

Again, as can be seen **Figure 24 (A)**, the NAcc was successfully reached, with a good level of infection. However, in comparison with **Figure 23,** we could clearly see that the infection was more widespread, reaching outside of the NAcc into the Accumbens shell. Furthermore, more areas of the mPFC, including the PrL and the Cg1, were infected (**Figure 24 (B)).** This difference between the two sets could be due to an injection site outside the NAcc, reaching the NAc shell. As this region is innervated by more regions of the mPFC [81] **(Figure 8)**, this could explain the more widespread infection observed. To better understand the specific connectivity within subregions of the mPFC and the NAcc, retrograding tracing experiments using Cholera SubToxin B must be performed.

We then tried to assess if our photo stimulation protocol was producing light-evoked neuronal activity. One possible technique to measure this is by detecting cFos expression. *cFos* is a proto-oncogene expressed on some neurons after depolarization, with its protein product identifiable by immunohistochemical techniques. As such, cFos expression might be used as a marker for neuronal activity [117–119]. Our photo stimulation protocol for cFos expression was designed such that only one hemisphere was stimulated. As seen in **Figure 25**, we could observe high cFos expression in the NAcc of both hemispheres. This suggests that there is ipsilateral and contralateral activation when photo-stimulation is performed.

Chapter V | Conclusion

In the course of this thesis, we found evidence that suggest that these two regions may encode winning information in the tube test setting. Furthermore, we were able to disrupt an already established social hierarchy by optogenetically activating these corticostriatal projections. Furthermore, we also found evidence that suggest that this change in rank can induce a "winner effect" in the stimulated mouse, winning trials even when not stimulated afterwards. However, this change was not long lasting, with the stimulated mouse returning to its initial rank after a few days.

Nonetheless, much of the present data shown here needs to be complemented with an increased number of animals and future experiments, such as retrograde tracing, in vitro electrophysiology as well as control optogenetic trials using only EYFP injection and different photo-stimulation protocols, modulating power intensity and frequency. Furthermore, it would also be of interest to assess if the "winner effect" observed was due to synaptic strengthening of corticostriatal projections and if modulating this synaptic efficiency would have any effect on a subject´s "winning streak".

Chapter VI | Supplementary Figures

Supplementary Figure 1 - Optical Fiber used

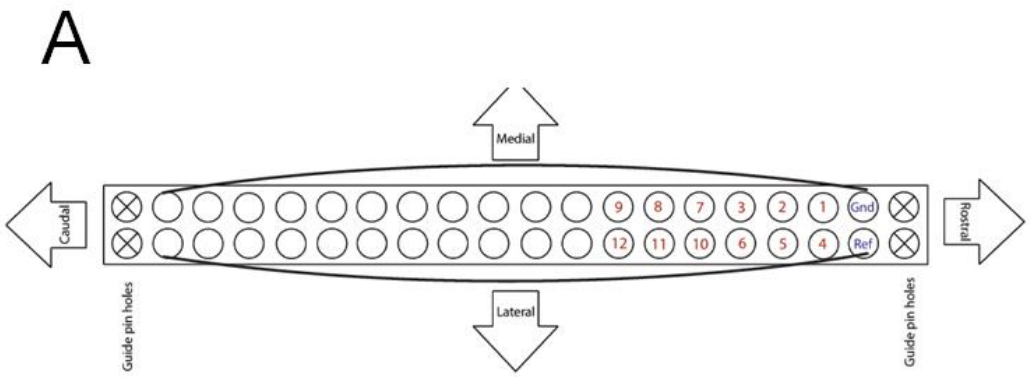

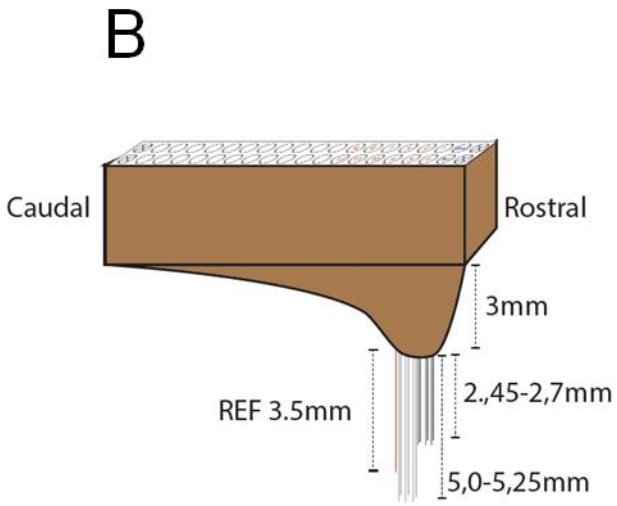

Supplementary Figure 2 – **(A)** Top view schematic of the MEA used **(B)** Schematic drawing of the MEA used kindly provided by Mário Carvalho

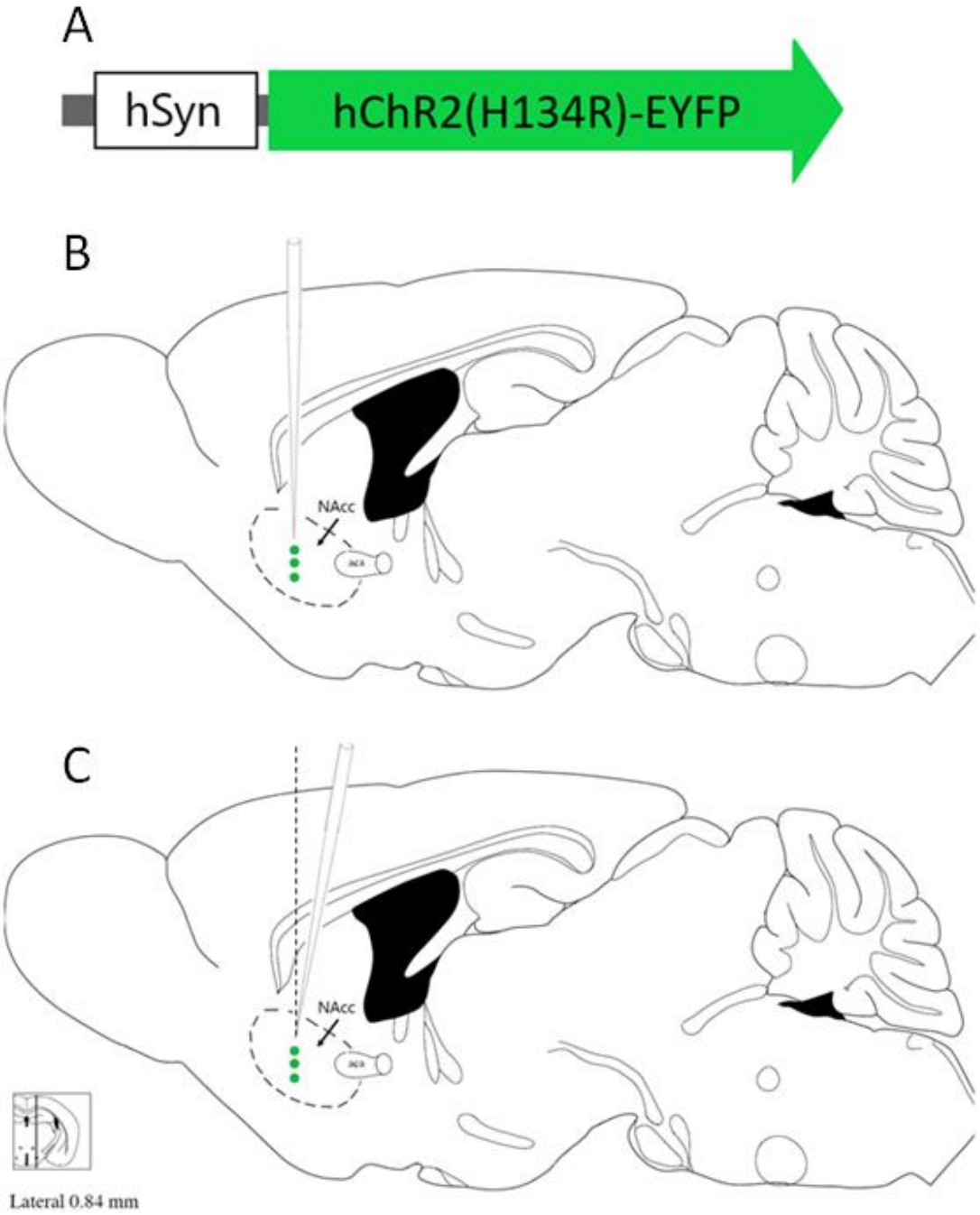

Supplementary Figure 3 – (A) AAV-hSyn-hChR2(H134R)-EYFP construct. **(B)** Schematic representation of the "0 degrees angle" Approach used for the viral construct delivery to the NAcc. **(C)** Schematic representation of the "10 degrees angle" Approach used for the viral construct delivery to the NAcc

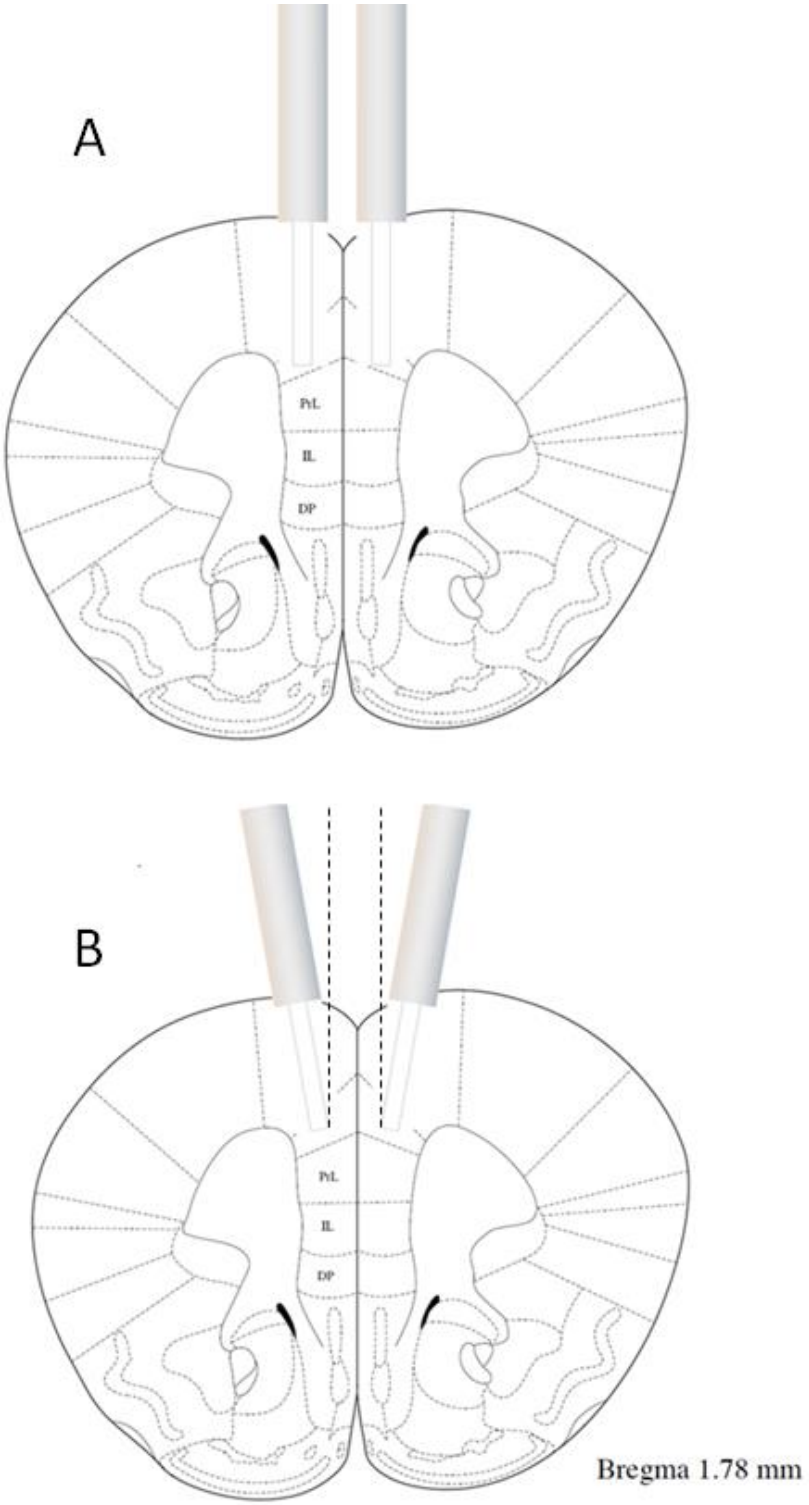

Supplementary Figure 4 – (A) Schematic representation of the “0 degrees angle” Approach used for the Optical Fibers Implantation. **(B)** Schematic representation of the “10 degrees angle” Approach used for the Optical Fibers Implantation

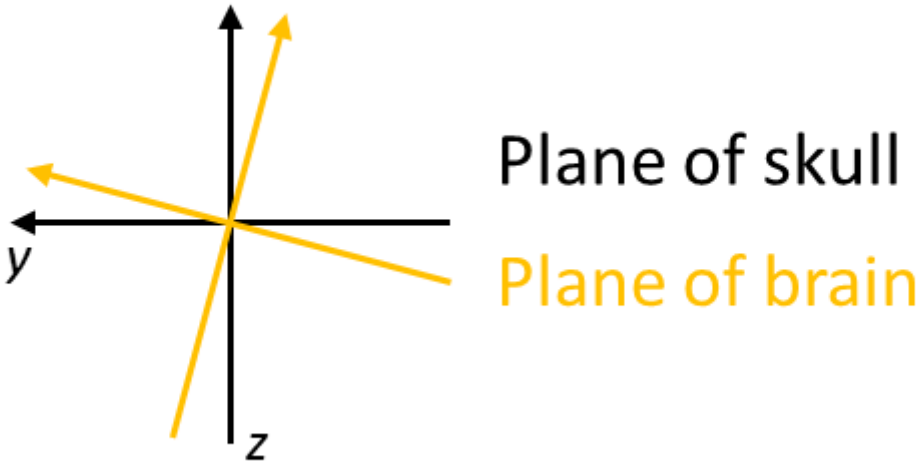

Supplementary Figure 5 – 15° slant of the skull relative to the brain

Chapter VII | References

1. Chase, I. D. Models of hierarchy formation in animal societies. *Behav. Sci.* **19,** 374–382 (1974).
2. Whitten, P. L. Diet and dominance among female vervet monkeys (Cercopithecus aethiops). *Am. J. Primatol.* **5,** 139–159 (1983).
3. Isbell, L. A., Pruetz, J. D., Lewis, M. & Young, T. P. Rank Differences in Ecological Behavior: A Comparative Study of Patas Monkeys (Erythrocebus patas) and Vervets (Cercopithecus aethiops). *Int. J. Primatol.* **20,** 257–272 (1999).
4. Breed, M. D., Smith, S. K. & Gall, B. G. Systems of mate selection in a cockroach species with male dominance hierarchies. *Anim. Behav.* **28,** 130–134 (1980).
5. Willisch, C. S. & Neuhaus, P. Social dominance and conflict reduction in rutting male Alpine ibex, Capra ibex. *Behav. Ecol.* **21,** 372–380 (2010).
6. Schjelderup-Ebbe, T. Observation on the social psychology of domestic fowls. *Z Psychol* 225–252 (1922).
7. Wilson, E. O. Sociobiology: The New Synthesis. *Harvard Univ. Press* **2000,**
8. Ostner, J., Nunn, C. L. & Schülke, O. Female reproductive synchrony predicts skewed paternity across primates. *Behav. Ecol.* **19,** 1150–1158 (2008).
9. Rodriguez-Llanes, J. M., Verbeke, G. & Finlayson, C. Reproductive benefits of high social status in male macaques (Macaca). *Anim. Behav.* **78,** 643–649 (2009).
10. Samuels, A., Silk, J. B. & Rodman, P. S. Changes in the Dominance Rank and Reproductive-Behavior of Male Bonnet Macaques (Macaca-Radiata). *Anim. Behav.* **32,** 994–1003 (1984).
11. Røskaft, E., Järvi, T., Bakken, M., Bech, C. & Reinertsen, R. E. The relationship between social status and resting metabolic rate in great tits (Parus major) and pied flycatchers (Ficedula hypoleuca). *Anim. Behav.* **34,** 838–842 (1986).
12. Martin, J. & Salvador, A. Tail loss reduces mating success in the Iberian rock-lizard, Lacerta monticola. *Behav. Ecol. Sociobiol.* **32,** 185–189 (1993).
13. Dittus, W. P. J. The Social Regulation of Population Density and Age-Sex Distribution in the Toque Monkey. *Behaviour* **63,** 281–322 (1977).
14. Owens, D. & Owens, M. Social dominance and reproductive patterns in brown hyaenas,Hyaena brunnea, of the central Kalahari desert. *Anim. Behav.* **51,** 535–551 (1996).
15. Ellis, L. Dominance and reproductive success among nonhuman animals: A cross-species comparison. *Ethol. Sociobiol.* **16,** 257–333 (1995).
16. Sapolsky, R. M. The Influence of Social Hierarchy on Primate Health. *Science (80-.).* **308,** 648–652 (2005).
17. Sapolsky, R. M. Testicular function, social rank and personality among wild baboons. *Psychoneuroendocrinology* **16,** 281–293 (1991).

18. Berry, R. J. The population genetics of the mouse. *Sci. Prog.* **64,** 341–370 (1977).
19. Singleton, G. R. & Krebs, C. J. The Secret World of Wild Mice. in *The Mouse in Biomedical Research* **1,** 25–51 (2007).
20. Van Loo, P. L. P., Mol, J. A., Koolhaas, J. M., Van Zutphen, B. F. M. & Baumans, V. Modulation of aggression in male mice: Influence of group size and cage size. *Physiol. Behav.* **72,** 675–683 (2001).
21. Shemesh, Y. *et al.* Correction: High-order social interactions in groups of mice. *Elife* **3,** e03602 (2014).
22. Kas, M. J. *et al.* Assessing behavioural and cognitive domains of autism spectrum disorders in rodents: Current status and future perspectives. *Psychopharmacology* **231,** 1125–1146 (2014).
23. ES Brodkin. BALB/c mice: low sociability and other phenotypes that may be relevant to autism. *Behav Brain Res* 53–65 (2007).
24. G. LINDZEY, H. W. & M. M. Social Dominance in Inbred Mouse Strains. *Nature* 474–476 (1961).
25. Wang, F. *et al.* Bidirectional control of social hierarchy by synaptic efficacy in medial prefrontal cortex. *Science* **334,** 693–7 (2011).
26. Chase, I., Tovey, C. & Murch, P. Two's Company, Three's a Crowd: Differences in Dominance Relationships in Isolated Versus Socially Embedded Pairs of Fish. *Behaviour* **140,** 1193–1217 (2003).
27. Seagraves, K. M., Arthur, B. J. & Egnor, S. E. R. Evidence for an audience effect in mice: male social partners alter the male vocal response to female cues. *J. Exp. Biol.* **219,** 1437–1448 (2016).
28. Dugatkin, L. A. Bystander effects and the structure of dominance hierarchies. *Behav. Ecol.* **12,** 348–352 (2001).
29. Hsu, Y. & Wolf, L. The winner and loser effect: integrating multiple experiences. *Anim. Behav.* **57,** 903–910 (1999).
30. Cummins, D. D. How the social environment shaped the evolution of mind. *Synthese* **122,** 3–28 (2000).
31. Chiao, J. Y. Neural basis of social status hierarchy across species. *Current Opinion in Neurobiology* **20,** 803–809 (2010).
32. Zink, C. F. *et al.* Know Your Place: Neural Processing of Social Hierarchy in Humans. *Neuron* **58,** 273–283 (2008).
33. Chou, M.-Y. *et al.* Social conflict resolution regulated by two dorsal habenular subregions in

zebrafish. *Science* **352,** 87–90 (2016).

34. Desban, L. & Wyart, C. A brain conditioned for social defeat. *Science (80-.).* **352,** 42–43 (2016).
35. Goldman-Rakic, P. S. The prefrontal landscape: implications of functional architecture for understanding human mentation and the central executive. *Philos Trans R Soc L. B Biol Sci* **351,** 1445–1453 (1996).
36. Mah, L., Arnold, M. C. & Grafman, J. Impairment of social perception associated with lesions of the prefrontal cortex. *Am. J. Psychiatry* **161,** 1247–1255 (2004).
37. Karafin, M. S., Tranel, D. & Adolphs, R. Dominance attributions following damage to the ventromedial prefrontal cortex. *J. Cogn. Neurosci.* **16,** 1796–1804 (2004).
38. Blair, R. J. R. & Cipolotti, L. Impaired social response reversal A case of 'acquired sociopathy'. *Brain* **123,** 1122–1141 (2000).
39. Bechara, A., Damasio, A. R., Damasio, H. & Anderson, S. W. Insensitivity to future consequences following damage to human prefrontal cortex. *Cognition* 7–15 (1994).
40. Anderson, S. W., Bechara, A., Damasio, H., Tranel, D. & Damasio, A. R. Impairment of social and moral behavior related to early damage in human prefrontal cortex. *Nat. Neurosci.* **2,** 1032–7 (1999).
41. Holson, R. R. Mesial prefrontal cortical lesions and timidity in rats. I. Reactivity to aversive stimuli. *Physiol. Behav.* **37,** 221–230 (1986).
42. Rudebeck, P. H. *et al.* Distinct contributions of frontal areas to emotion and social behaviour in the rat. *Eur. J. Neurosci.* **26,** 2315–2326 (2007).
43. Mitchell, J. P. Contributions of functional neuroimaging to the study of social cognition. *Curr. Dir. Psychol. Sci.* **17,** 142–146 (2008).
44. Spreng, R. N., Mar, R. A. & Kim, A. S. N. The Common Neural Basis of Autobiographical Memory, Prospection, Navigation, Theory of Mind, and the Default Mode: A Quantitative Meta-analysis. *J. Cogn. Neurosci.* **21,** 489–510 (2008).
45. Wagner, D. D., Haxby, J. V. & Heatherton, T. F. The representation of self and person knowledge in the medial prefrontal cortex. *Wiley Interdisciplinary Reviews: Cognitive Science* **3,** 451–470 (2012).
46. Moran, J. M., Jolly, E. & Mitchell, J. P. Social-Cognitive Deficits in Normal Aging. *J. Neurosci.* **32,** 5553–5561 (2012).
47. Spunt, R. P. & Adolphs, R. Folk Explanations of Behavior: A Specialized Use of a Domain-General Mechanism. *Psychol. Sci.* **26,** 724–736 (2015).
48. Ferrari, C., Vecchi, T., Todorov, A. & Cattaneo, Z. Interfering with activity in the dorsomedial

prefrontal cortex via tms affects social impressions updating. *Cogn. Affect. {&} Behav. Neurosci.* No Pagination Specified (2016). doi:10.3758/s13415-016-0419-2

49. Wagner, D. D., Kelley, W. M., Haxby, J. V. & Heatherton, T. F. The Dorsal Medial Prefrontal Cortex Responds Preferentially to Social Interactions during Natural Viewing. *J. Neurosci.* **36,** 6917–6925 (2016).
50. Tingting Zhou, Hong Zhu, Zhengxiao Fan, Fei Wang, Yang Chen, H. L. History of winning remodels thalamo-PFC circuit to reinforce social dominance. *Science (80-.).* **357,** 162–168 (2017).
51. Lee, E. *et al.* Enhanced Neuronal Activity in the Medial Prefrontal Cortex during Social Approach Behavior. *J. Neurosci.* **36,** 6926–6936 (2016).
52. Euston, D. R., Gruber, A. J. & McNaughton, B. L. The Role of Medial Prefrontal Cortex in Memory and Decision Making. *Neuron* **76,** 1057–1070 (2012).
53. Tse, D. *et al.* Schema-dependent gene activation and memory encoding in neocortex. *Science* **333,** 891–5 (2011).
54. Wang, F., Kessels, H. W. & Hu, H. The mouse that roared: Neural mechanisms of social hierarchy. *Trends in Neurosciences* **37,** 674–682 (2014).
55. Felix-Ortiz, A. C., Burgos-Robles, A., Bhagat, N. D., Leppla, C. A. & Tye, K. M. Bidirectional modulation of anxiety-related and social behaviors by amygdala projections to the medial prefrontal cortex. *Neuroscience* **321,** 197–209 (2016).
56. Matsumoto, M. & Hikosaka, O. Two types of dopamine neuron distinctly convey positive and negative motivational signals. *Nature* **459,** 837–841 (2009).
57. Apicella, P., Scarnati, E., Ljungberg, T. & Schultz, W. Neuronal activity in monkey striatum related to the expectation of predictable environmental events. *J Neurophysiol* **68,** 945–960 (1992).
58. Tremblay, L., Hollerman, J. R. & Schultz, W. Modifications of reward expectation-related neuronal activity during learning in primate striatum. *J. Neurophysiol.* **80,** 964–977 (1998).
59. Groenewegen, H. J., Wright, C. I. & Uylings, H. B. The anatomical relationships of the prefrontal cortex with limbic structures and the basal ganglia. *J. Psychopharmacol.* **11,** 99–106 (1997).
60. Fliessbach, K. *et al.* Social comparison affects reward-related brain activity in the human ventral striatum. *Science* **318,** 1305–8 (2007).
61. Bault, N., Joffily, M., Rustichini, A. & Coricelli, G. Medial prefrontal cortex and striatum mediate the influence of social comparison on the decision process. *Proc. Natl. Acad. Sci.* **108,** 16044–9 (2011).

62. Tom, S. M., Fox, C. R., Trepel, C. & Poldrack, R. a. The neural basis of loss aversion in decision-making under risk. *Science* **315,** 515–518 (2007).
63. Watanabe, N., Sakagami, M. & Haruno, M. Reward prediction error signal enhanced by striatum-amygdala interaction explains the acceleration of probabilistic reward learning by emotion. *J Neurosci* **33,** 4487–4493 (2013).
64. Delgado, M. R., Gillis, M. M. & Phelps, E. a. Regulating the expectation of reward via cognitive strategies. *Nat. Neurosci.* **11,** 880–1 (2008).
65. Ly, M., Haynes, M. R., Barter, J. W., Weinberger, D. R. & Zink, C. F. Subjective socioeconomic status predicts human ventral striatal responses to social status information. *Curr. Biol.* **21,** 794–797 (2011).
66. Morgan, D. *et al.* Social dominance in monkeys: dopamine D-2 receptors and cocaine self-administration. *Nat. Neurosci.* **5,** 169–174 (2002).
67. Báez-Mendoza, R. & Schultz, W. Performance error-related activity in monkey striatum during social interactions. *Sci. Rep.* **6,** 37199 (2016).
68. Smith, Y., Wichmann, T. & DeLong, M. R. Corticostriatal and mesocortical dopamine systems: do species differences matter? *Nat. Rev. Neurosci.* **15,** 63 (2014).
69. Ferino, F., Thierry, A. M., Saffroy, M. & Glowinski, J. Interhemispheric and subcortical collaterals of medial prefrontal cortical neurons in the rat. *Brain Res.* **417,** 257–266 (1987).
70. Wilson, C. J. Morphology and synaptic connections of crossed corticostriatal neurons in the rat. *J. Comp. Neurol.* **263,** 567–580 (1987).
71. Lévesque, M., Charara, A., Gagnon, S., Parent, A. & Deschênes, M. Corticostriatal projections from layer V cells in rat are collaterals of long-range corticofugal axons. *Brain Res.* **709,** 311–315 (1996).
72. Dias-Ferreira, E. *et al.* Chronic Stress Causes Frontostriatal Reorganization and Affects Decision-Making. *Science (80-.).* **325,** 621–625 (2009).
73. Shepherd, G. M. G. Corticostriatal connectivity and its role in disease. *Nat. Rev. Neurosci.* **14,** 278–91 (2013).
74. Kita, T. & Kita, H. The subthalamic nucleus is one of multiple innervation sites for long-range corticofugal axons: a single-axon tracing study in the rat. *J. Neurosci.* **32,** 5990–9 (2012).
75. Morishima, M. Recurrent Connection Patterns of Corticostriatal Pyramidal Cells in Frontal Cortex. *J. Neurosci.* **26,** 4394–4405 (2006).
76. Brown, S. P. & Hestrin, S. Intracortical circuits of pyramidal neurons reflect their long-range axonal targets. *Nature* **457,** 1133–1136 (2009).
77. Kiritani, T., Wickersham, I. R., Seung, H. S. & Shepherd, G. M. G. Hierarchical Connectivity and

Connection-Specific Dynamics in the Corticospinal-Corticostriatal Microcircuit in Mouse Motor Cortex. *J. Neurosci.* **32,** 4992–5001 (2012).

78. Douglas, R. J., Koch, C., Mahowald, M., Martin, K. a & Suarez, H. H. Recurrent excitation in neocortical circuits. *Science (80-.).* **269,** 1–5 (1995).
79. Lübke, J., Egger, V., Sakmann, B. & Feldmeyer, D. Columnar organization of dendrites and axons of single and synaptically coupled excitatory spiny neurons in layer 4 of the rat barrel cortex. *J. Neurosci.* **20,** 5300–11 (2000).
80. Wang, X.-J. Neurophysiological and computational principles of cortical rhythms in cognition. *Physiol. Rev.* **90,** 1195–268 (2010).
81. André, V. M. *et al. Handbook of Basal Ganglia Structure and Function*. *Handbook of Behavioral Neuroscience* **20,** (2010).
82. Phillipson, O. T. *et al.* Selective presynaptic enhancement of the prefrontal cortex to nucleus accumbens pathway by cocaine. *Pnas* **110,** 713–8 (2013).
83. Britt, J. P. *et al.* Synaptic and Behavioral Profile of Multiple Glutamatergic Inputs to the Nucleus Accumbens. *Neuron* **76,** 790–803 (2012).
84. Lee, A. T., Vogt, D., Rubenstein, J. L. & Sohal, V. S. A class of GABAergic neurons in the prefrontal cortex sends long-range projections to the nucleus accumbens and elicits acute avoidance behavior. *J. Neurosci.* **34,** 11519–25 (2014).
85. Floresco, S. B., Braaksma, D. N. & Phillips, a G. Thalamic-cortical-striatal circuitry subserves working memory during delayed responding on a radial arm maze. *J. Neurosci.* **19,** 11061–11071 (1999).
86. Hauber, W. & Sommer, S. Prefrontostriatal circuitry regulates effort-related decision making. *Cereb. Cortex* **19,** 2240–2247 (2009).
87. Christakou, A., Robbins, T. W. & Everitt, B. J. Prefrontal Cortical-Ventral Striatal Interactions Involved in Affective Modulation of Attentional Performance: Implications for Corticostriatal Circuit Function. *J. Neurosci.* **24,** 773–780 (2004).
88. Rogers, R. D., Baunez, C., Everitt, B. J. & Robbins, T. W. Lesions of the medial and lateral striatum in the rat produce differential deficits in attentional performance. *Behav Neurosci* **115,** 799–811 (2001).
89. Amadei, E. A. *et al.* Dynamic corticostriatal activity biases social bonding in monogamous female prairie voles. *Nature* **546,** 297–301 (2017).
90. Sparta, D. R. *et al.* Construction of implantable optical fibers for long-term optogenetic manipulation of neural circuits. *Nat. Protoc.* **7,** 12–23 (2012).
91. Cetin, A., Komai, S., Eliava, M., Seeburg, P. H. & Osten, P. Stereotaxic gene delivery in the

rodent brain. *Nat. Protoc.* **1,** 3166–73 (2006).

92. Paxinos, G., Franklin, K. B. J., Paxinos, G and Franklin, K. B. J., Paxinos, G. & Franklin, K. B. J. *Mouse Brain in Stereotaxic Coordinates*. *Academic Press* **2nd,** (2004).
93. Morgan, C. W., Julien, O., Unger, E. K., Shah, N. M. & Wells, J. A. Turning on caspases with genetics and small molecules. *Methods Enzymol.* **544,** 179–213 (2014).
94. Mitzdorf, U. Current source-density method and application in cat cerebral cortex: investigation of evoked potentials and EEG phenomena. *Physiol. Rev.* **65,** 37–100 (1985).
95. Einevoll, G. T., Kayser, C., Logothetis, N. K. & Panzeri, S. Modelling and analysis of local field potentials for studying the function of cortical circuits. *Nat. Rev. Neurosci.* **14,** 770–85 (2013).
96. Di, S., Baumgartner, C. & Barth, D. S. Laminar analysis of extracellular field potentials in rat vibrissa/barrel cortex. *J. Neurophysiol.* **63,** 832–40 (1990).
97. Barth, D. S. & Di, S. Laminar excitability cycles in neocortex. *J. Neurophysiol.* **65,** 891–898 (1991).
98. Kandel, a & Buzsáki, G. Cellular-synaptic generation of sleep spindles, spike-and-wave discharges, and evoked thalamocortical responses in the neocortex of the rat. *J. Neurosci.* **17,** 6783–6797 (1997).
99. Scherberger, H., Jarvis, M. R. & Andersen, R. A. Cortical local field potential encodes movement intentions in the posterior parietal cortex. *Neuron* **46,** 347–354 (2005).
100. Roux, S., MacKay, W. A. & Riehle, A. The pre-movement component of motor cortical local field potentials reflects the level of expectancy. *Behav. Brain Res.* **169,** 335–351 (2006).
101. Pesaran, B., Pezaris, J. S., Sahani, M., Mitra, P. P. & Andersen, R. a. Temporal structure in neuronal activity during working memory in macaque parietal cortex. *Nat. Neurosci.* **5,** 805–811 (2002).
102. Kreiman, G. *et al.* Object selectivity of local field potentials and spikes in the macaque inferior temporal cortex. *Neuron* **49,** 433–445 (2006).
103. Seidenbecher, T., Laxmi, T. R., Stork, O. & Pape, H.-C. Amygdalar and hippocampal theta rhythm synchronization during fear memory retrieval. *Science* **301,** 846–50 (2003).
104. Pape, H. C., Narayanan, R. T., Smid, J., Stork, O. & Seidenbecher, T. Theta activity in neurons and networks of the amygdala related to long-term fear memory. *Hippocampus* **15,** 874–880 (2005).
105. Zhang, F. *et al.* Optogenetic interrogation of neural circuits: technology for probing mammalian brain structures. *Nat. Protoc.* **5,** 439–56 (2010).
106. Gradinaru, V., Mogri, M., Thompson, K. R., Henderson, J. M. & Deisseroth, K. Optical deconstruction of parkinsonian neural circuitry. *Science* **324,** 354–9 (2009).

107. Gradinaru, V. *et al.* Targeting and readout strategies for fast optical neural control in vitro and in vivo. *J. Neurosci.* **27,** 14231–14238 (2007).
108. Lee, J. H. *et al.* Global and local fMRI signals driven by neurons defined optogenetically by type and wiring. *Nature* **465,** 788–792 (2010).
109. Petreanu, L., Huber, D., Sobczyk, A. & Svoboda, K. Channelrhodopsin-2-assisted circuit mapping of long-range callosal projections. *Nat. Neurosci.* **10,** 663–8 (2007).
110. Wesson, D. W. Sniffing behavior communicates social hierarchy. *Curr. Biol.* **23,** 575–580 (2013).
111. Bonabeau, E., Theraulaz, G. & Deneubourg, J. L. Dominance orders in animal societies: the self-organization hypothesis revisited. *Bull. Math. Biol.* **61,** 727–757 (1999).
112. Kura, K., Broom, M. & Kandler, A. A Game-Theoretical Winner and Loser Model of Dominance Hierarchy Formation. *Bull. Math. Biol.* **78,** 1259–1290 (2016).
113. Nabavi, S. *et al.* Engineering a memory with LTD and LTP. *Nature* **511,** 348–352 (2014).
114. Pascoli, V., Turiault, M. & Lüscher, C. Reversal of cocaine-evoked synaptic potentiation resets drug-induced adaptive behaviour. *Nature* **481,** 71–5 (2011).
115. Cardin, J. a *et al.* Driving fast-spiking cells induces gamma rhythm and controls sensory responses. *Nature* **459,** 663–7 (2009).
116. Cardin, J. A. *et al.* Targeted optogenetic stimulation and recording of neurons in vivo using cell-type-specific expression of Channelrhodopsin-2. *Nat. Protoc.* **5,** 247–54 (2010).
117. Bullitt, E. Expression of c-fos-like protein as a marker for neuronal activity following noxious stimulation in the rat. *J. Comp. Neurol.* **296,** 517–530 (1990).
118. Dragunow, M. & Faull, R. The use of c-fos as a metabolic marker in neuronal pathway tracing. *J. Neurosci. Methods* **29,** 261–265 (1989).
119. Day, H. E. W., Kryskow, E. M., Nyhuis, T. J., Herlihy, L. & Campeau, S. Conditioned fear inhibits c-fos mRNA expression in the central extended amygdala. *Brain Res.* **1229,** 137–146 (2008).